AD-A036 272 DELAWARE UNIV NEWARK DEPT OF CIVIL ENGINEERING F/G 8/10
COMPUTER MODEL FOR ENERGY SPECTRUM TRANSFORMATION OVER IRREGULA--ETC(U)
JUL 76 H WANG, J C SHIAU N00014-76-C-0342
UNCLASSIFIED OCEAN ENGINEERING-9 NL

| OF |
AD
A036272

END

DATE
FILMED
3-77

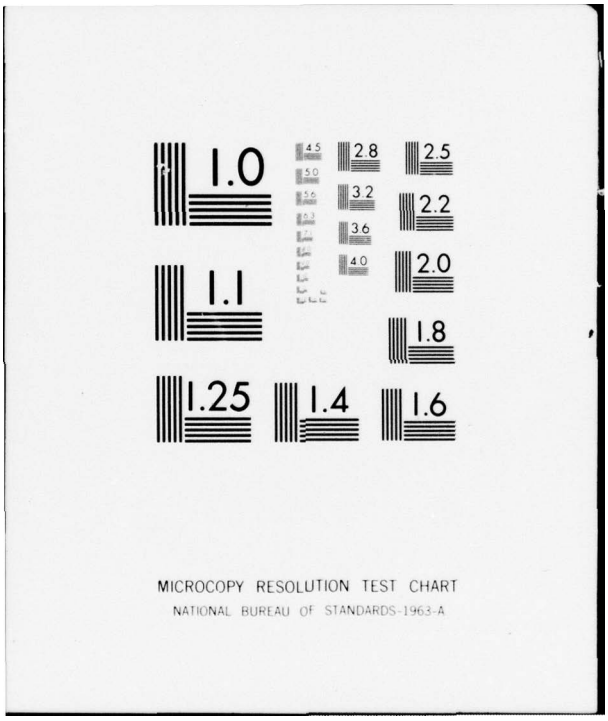
1.0
1.1
1.25
1.4
1.6
1.8
2.0
2.2
2.5
2.8
3.2
3.6
4.0
4.5
5.0
5.6
6.3
MICROCOPY RESOLUTION TEST CHART
NATIONAL BUREAU OF STANDARDS-1963-A

Computer Model for Energy Spectrum Transformation Over Irregular Bottom Topography

by

Hsiang Wang

and

J. C. Shiau

Technical Report No. 2

Contract No. N0014-76-C-0342
with the
OFFICE OF NAVAL RESEARCH GEOGRAPHY PROGRAMS

Ocean Engineering Report No. 9

July 1976

Department of Civil Engineering
University of Delaware
Newark, Delaware

COMPUTER MODEL FOR ENERGY SPECTRUM TRANSFORMATION OVER IRREGULAR BOTTOM TOPOGRAPHY

by

Hsiang Wang

and

J. C. Shiau

Technical Report No. 2

Contract No. N0014-76-C-0342
with the
OFFICE OF NAVAL RESEARCH GEOGRAPHY PROGRAMS

Ocean Engineering Report No. 9

July 1976

Department of Civil Engineering
University of Delaware
Newark, Delaware

TABLE OF CONTENTS

ACKNOWLEDGMENTS

This work was supported by the Office of Naval Research Geographic Programs, Contract No. N0014-76-C-0342. The many helpful comments made by Dr. Robert G. Dean are acknowledged here. The manuscript was prepared while the first author was at the Leichtweiss-Institut für Wasserbau, der Technischen Universitat Braunschweig, Germany, partially under the sponsorship of Minna-James-Heineman Stiftung.

LIST OF FIGURES

LIST OF SYMBOLS

A_o	amplitude of shoreline undulation
e	wave phase velocity = L/T
C_g	wave group velocity
E	wave energy
f_i	index column for rhythmic topography
F	spectral density function
g	gravitational acceleration
h	local water depth
h_b	water depth at wave breaking point
h_o	elevation at the origin of coordinate system
H	wave height
i	grid index x-direction
j	grid index y-direction
k	magnitude of the wave number = $2\pi/L$
k_o	deepwater wave number
$K(\theta)$	directional spreading function for wave energy
L	wave length
m	beach slope
r	magnitude of position vector
$\vec{r}$	position vector
S	extent in offshore direction where bottom undulation begins, beyond which the contour is parallel
$S(\omega)$	one-dimensional spectral density function
t	time

List of Symbols (Continued)

T	wave period
u	wind speed
x	coordinate perpendicular to shoreline
y	coordinate parallel to shoreline
Δx	grid size in x-direction
Δy	grid size in y-direction
α	polar angle of the spectral vector
γ	specific weight of fluid
θ	wave direction
ξ	dummy variable
ϕ	the frequency directional wave spectral density function
ϕ_o	deepwater frequency, directional wave spectral density function
ω	wave angular frequency = $2\pi/T$

ABSTRACT

Based on the assumption that the wave energy associated with a narrow frequency band stayed within the band upon refraction, a numerical model based on finite difference method has been developed. This model, utilizing electronic computer, proves to be quite convenient to determine shallow water wave spectra at designated spatial locations of irregular bottom contours provided the deepwater wave spectrum is given. The model has been verified against analytical solution for case of two-dimensional parallel bottom contours and compared in good agreement with field measurement at location well beyond the surf zone.

CHAPTER I INTRODUCTION

The needs for more realistic representation and accurate prediction of sahllow water environment are increasing for both scientific and engineering purposes, in particular, due to the advent of anticipated continental shelf development. It is also an accepted opinion that wave spectrum which utilizes the ensemble of random surface oscillations provides a more realistic, and perhaps more accurate, representation of ocean waves than monochromatic wave train of regular oscillation. In the past, considerable efforts have been devoted in the development of deep water wave spectrum to the extent that one has reasonable confidence on its applicability to describe wind generated ocean waves. The goal of this work is to develop a practical method of transforming this deepwater water wave spectra into shallow water of irregular bottom topography.

A number of investigators (Longuet-Higgins, 1956; Collins, 1970; etc.) have studied the theoretical formulation of the transformation of wind wave spectrum in shoaling water by considering the conservation of energy between adjacent wave rays much the same way of the wave refraction in monocromatic wave train. Based on Longuet-Higgins' formulation, Karlesson (1969) developed a method to compute spectrum transformation over parallel bottom contours. Collins (1972) extended the work to the inclusion of bottom friction and have mentioned the application to the irregular bottom topography. However, his numerical scheme traces wave energy along wave rays which makes the computational procedure quite

impractical in determining shallow water wave spectrum at designated locations over an area of irregular offshore bottom configuration. More recently, Krasitkiy (1974) has derived explicit analytical solutions for the spectrum transformation over two-dimensional parallel bottom contrours.

The present study presents a numerical method which proves to be effective to transform deepwater wave spectrum into shallow water regions. It is based on the assumption that the wave energy associated with a narrow frequency band stays within this band upon refraction when waves propagate from deep into shallow waters. A recently developed wave refraction program (Noda, et al., 1974) is modified to compute the spatial modification of the incident wave energy within the designated frequency. The shallow water wave spectrum at any specified location, is then simply the contributions resulting from energy associated with different frequency bands of the spectrum.

Examples of the spectrum distribution over parallel bottom contours, irregular bottom bathymetry and rhythmic topography were illustrated. Comparisons of the present results with analytic solution obtained by Krasitskiy and the field observations were made.

CHAPTER II TRANSFORMATION OF ENERGY SPECTRUM

Let $F(k,r,t)$ be the spectral density function defined as energy per unit area per unit wave number space, the total energy is equal to the summation of the spectral density over the whole wave number space, i.e.,

$$E = \int_0^\infty F(k,\vec{r},t)dk \tag{1}$$

where k = magnitude of the wave number = $2\pi/L$

L = wave length

$\vec{r}$ = position vector

t = time

For the case of steady state, the wave energy contained within a small increment dk can be expressed as

$$\Delta E = \int_k^{k+dk} F(\xi,\vec{r})d\xi$$

Through Taylor's expansion and neglecting higher orders, we have

$$\Delta E = F(k,\vec{r})dk \tag{2}$$

It is known that for linear wave systems, the following dispersion relationship exists

$$\omega^2 = gk \text{ Tanh } kh \tag{3}$$

where ω = wave angular frequency = $2\pi/T$

T = wave period

h = local water depth

g = gravitational acceleration

Differentiating the above equation results in

$$d\omega = C_g\, dk \tag{4}$$

where C_g = wave group velocity = nc

$n = (1 + 2kh/\sinh 2kh)/2$

c = wave phase velocity = L/T

Utilizing the above relation, the wave number spectral density function $F(k,\vec{r})$ can be transformed into polar frequency direction space as

$$F(k,r) = \frac{Cg}{k}\ \phi(\omega, \alpha, r) \tag{5}$$

where ϕ = the frequency directional wave spectral density function

r = magnitude of space vector $\vec{r}$

α = polar angle of the spectral vector

Combining Equations (2) and (5), one obtains

$$\phi(\omega,\alpha,r) = \frac{k\Delta E}{d\omega} \tag{6}$$

Assuming that the wave energy associated with a narrow frequency band would stay within this band upon wave refraction, a relationship between shallow water and deepwater wave energy spectra can be obtained by

$$\phi = \frac{k}{k_o}\frac{\Delta E}{\Delta E_o}\phi_o \tag{7}$$

where the subscript o denotes deepwater conditions.

For small amplitude waves, it is known that (Lamb, 1932)

$$E = \gamma \cdot \frac{H^2}{8}$$

where γ = specific weight of the fluid

H = wave height

It is plausible to assume here that

$$\Delta E = \gamma \cdot \frac{(\Delta H)^2}{8} \tag{8}$$

where ΔH can be interpreted as the contribution to the total wave height due to the associated increment of wave energy. Based on this relationship, Equation (7) can be rewritten as

$$\phi = \frac{k}{k_o} \frac{(\Delta H)^2}{(\Delta H_o)^2} \phi_o \tag{9}$$

This equation which clearly reveals the effects of shoaling and dispersion is the key equation for wave energy transformation computations. It is evident from this equation that the task of computing ϕ requires the computation of wave height and wave number transformations at designated locations.

CHAPTER III TRANSFORMATION OF WAVE CLIMATE

To compute wave height and wave number transformation at designated locations in shallow water, a numerical program on wave refraction and shoaling recently developed by Noda et.al. (1974) is adopted and modified. This method like most of the existing techniques in computing wave refraction, neglected the nonlinear effects, bottom friction, turbulent dissipation and bottom percolation. The procedure involves solving a pair of simultaneous equations for the wave direction and the wave height. The first equation is derived from the fact that the wave number vector field, k, is irrotational (Phillips, 1966). In Cartesian coordinates as shown in Figure 1, the following equation results

$$\cos\theta \frac{\partial\theta}{\partial x} + \sin\theta \frac{\partial\theta}{\partial y} = \frac{1}{k}\left(\cos\theta \frac{\partial k}{\partial y} - \sin\theta \frac{\partial k}{\partial x}\right) \tag{10}$$

where θ = angle of wave incidence to the beach normal

x = Cartesian coordinate perpendicular to the shoreline

y = Cartesian coordinate parallel to the shoreline

The partial derivatives of k were determined from the wave dispersion relationship expressed in Equation (3). The second equation is obtained from the condition of the steady state conservation of energy (Phillips, 1966).

$$(C_g \cos\theta)\frac{2}{H}\frac{\partial H}{\partial x} + (C_g \sin\theta)\frac{2}{H}\frac{\partial H}{\partial y} + \cos\theta \frac{\partial C_g}{\partial x} - C_g \sin\theta \frac{\partial\theta}{\partial x} + \sin\theta \frac{\partial C_g}{\partial y} + C_g \cos\theta \frac{\partial\theta}{\partial y} = 0 \tag{11}$$

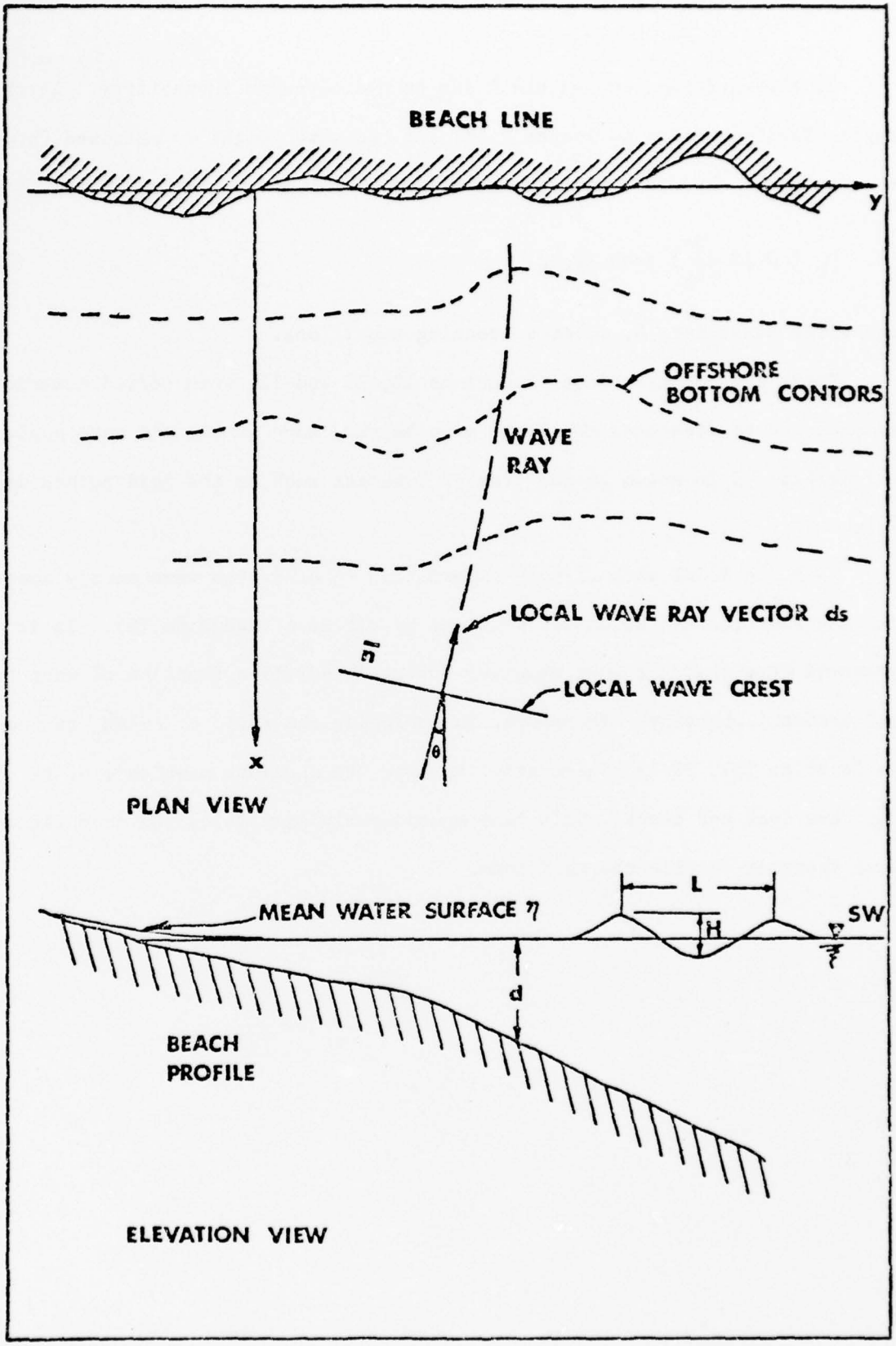

Figure 1 Definition Sketch of Nearshore Environment

In the surf zone, waves break due to hydrodynamic instability. In this region Equation 11 is no longer valid and the wave height is obtained through the use of an empirical equation developed by LeMehaute and Koh (1967).

$$H_b = 0.12 \left(\frac{2\pi}{k_b}\right) \tanh (k_b h_b) \tag{12}$$

where the subscript, b, denotes breaking conditions.

These sets of equations, Equations 10, 11 and 12, when solved numerically, enables one to determine the local wave height, wave number and wave angle at any designated location in the area of interest such as the grid points in Figure 2.

With the local wave climate information in hand, the wave energy spectral density function can be easily obtained by virtue of Equation (9). It is observed here that the wave shoaling effect is purely a function of wave frequency and bottom topography. Therefore, in computing the ratio of $\Delta H/\Delta H_o$ as required in Equation (9), it is nonessential to know the absolute magnitude of ΔH_o provided the wave does not break. This fact considerably simplifies the computation of wave spectrum outside the surf zone.

CHAPTER IV NUMERICAL PROCEDURES

Computational Scheme. The computation of the transformation of wave climate follows closely the method developed by Noda (1974). Equations of (10) and (11) are written in finite difference form using a forward difference in x, and a backward difference in y for the local grid system shown in Figure 3. Each grid was assigned a mean depth h_{ij} and an area $\Delta x\ \Delta y$. All major quantities--H, θ, k--are computed at the grid center. Values of $\sin\theta_{i,j}$ and $\cos\theta_{i,j}$ are determined using an average of these quantities from four surrounding grid blocks approximated to second order in a Taylor series expansion, i.e.,

$$\sin\theta_{i,j} = \frac{1}{4}\left(\sin\theta_{i+1,j} + \sin\theta_{i-1,j} + \sin\theta_{i,j+1} + \sin\theta_{i,j-1}\right)$$

$$+ \frac{1}{8}\left[(\theta_{i+1,j} - \theta_{i-1,j})(\cos\theta_{i-1,j} - \cos\theta_{i+1,j}) + (\theta_{i,j+1} - \theta_{i,j-1})\right.$$

$$\left.(\cos\theta_{i,j+1} - \cos\theta_{i,j-1})\right] \qquad (13)$$

etc.

The numerical iterations are carried to an acceptable error, in this case,

$$\frac{|X_{new} - X_{old}|}{|X_{new}|} \leq 0.1\% \qquad (14)$$

where X represents all the variables under consideration.

The computation of spectrum transformation does not involve numerical integration and is straight forward from Equation (9).

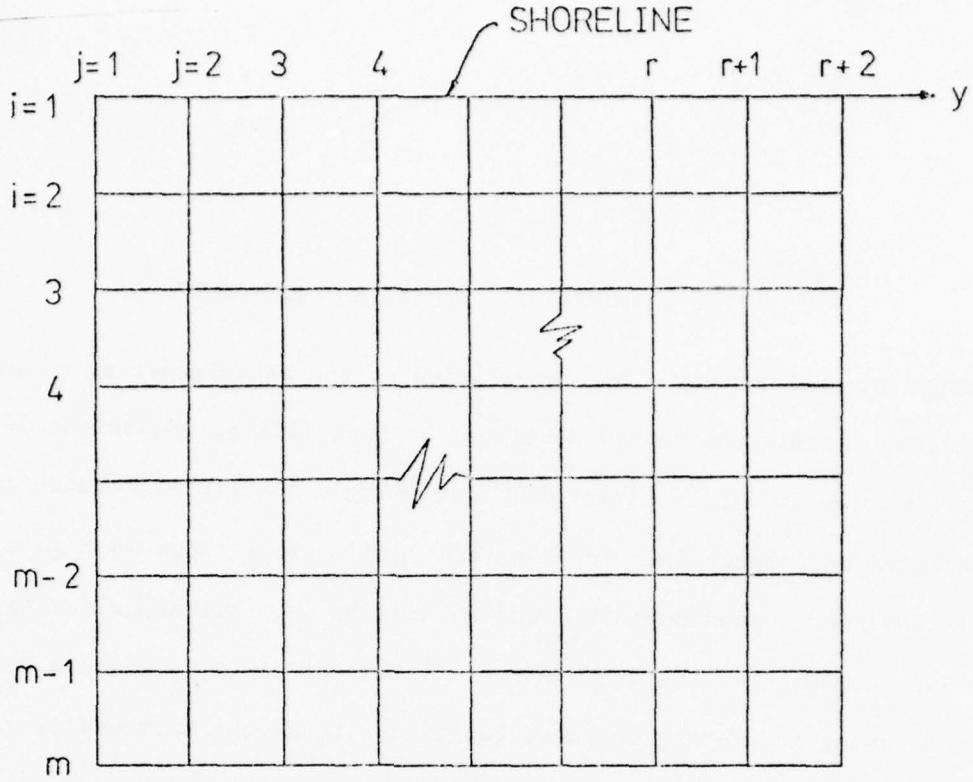

Figure 2 Grid System Used in Computation

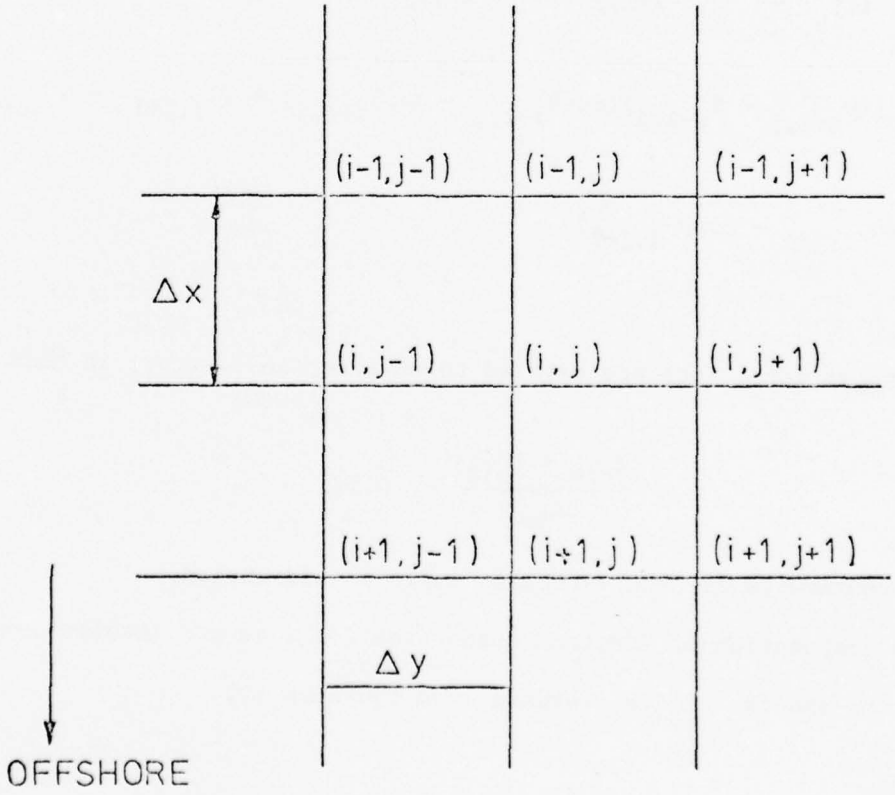

Figure 3 Local Grid Description

Boundary Conditions. The condition at the shoreward boundary is simply that the wave angles are normal to the shoreline at the boundary. Two different options are built in the program for the side boundaries.

A. For rhythmic topography--In this case the wave condition repeats itself at space intervals equal to the integer multiplications of the periodic length. The boundary condition can be self-generated by adding additional grid column such that

$$f_{i,\ N+1} = f_{i,2} \tag{15}$$

where N+1 = periodic length.

A. For slowly varying irregular topography--The conditions at the upwave side are computed by extending the bottom profiles two dimensionally such that the wave refraction follow the Snell law up to the boundary. The downward side boundary condition needs not be prescribed for this case.

Input Wave Condition. Strictly speaking, directional spectrum of the form $\phi_B(\omega,\theta)$ should be prescribed at the seaward boundary. Since our present knowledge on directional spectrum is quite inadequate, the program, therefore, is written to accept the deepwater wave spectrum of the following form as input:

$$\phi_o\ (\omega,\theta) = S(\omega)\ K(\theta) \tag{16}$$

where $K(\theta)$ is an artificial weighting function to estimate the effect of directional spreading. For the sample computations to be illustrated $S(\omega)$ is taken to be the Pierson-Moskowitz's deep water wave spectrum:

$$S(\omega) = \alpha \frac{g^2}{\omega^5} \exp\left[-\beta \left(\frac{g}{\omega U}\right)^4\right] \tag{17}$$

where U is the wind speed, $\alpha = 8.1 \times 10^{-3}$ and $\beta = 0.74$.

The function of $K(\theta)$ assumes the form of

$$K(\theta) = \begin{cases} (8/3\pi)\cos^4\theta & |\theta| < \pi/2 \\ 0 & |\theta| \geq \pi/2 \end{cases} \tag{18}$$

to facilitate comparisons with analytical results of Krasitskiy (1974).

As the seaward boundary is often set at finite water depths to avoid excessive computational time the deep water wave spectrum is transformed to the finite depths at the boundary using analytical solution of Krasitskiy (1974) with the assumption that the offshore topography can be approximated by two-dimensional parallel contours.

CHAPTER V VERIFICATION AND APPLICATIONS

Sample computations of three different types of bottom hydrographs are illustrated here. The first example is for a two-dimensional parallel contour case such that the results can be compared with analytical solution of Krasitskiy (1974). The calculations are carried out for a wind speed of 20.5m/sec (the same value chosen by Krasitskiy) and a uniform slope m = 0.005. Figure 4 compares the numerical results of spectral density function with the analytical ones for water depths of ∞, 25M and 15M. The present numerical scheme yields satisfactory results except at high frequency end where small deviations from the analytical values are noted. This discrepancy is considered inevitable due to the finite grid size. Reducing grid size will improve the numerical errors at the expense of increasing computational time.

The second case is a comparison between computed spectrum with the field measurements. The spectrum transformation along the Delaware coast, facing the Atlantic Ocean, located approximately two miles north of Indian River Inlet (Figure 5) was examined. Field measurements were obtained by capacitance-type wave gage mounted on a wave tower in water of approximately 4.4m deep. The location of the tower and the bottom bathymetry is shown in Figure 6. Data was recorded on tape. Wave energy spectrum was obtained through fast-Fourier analysis. Detailed descriptions of the field measuring program is documented by

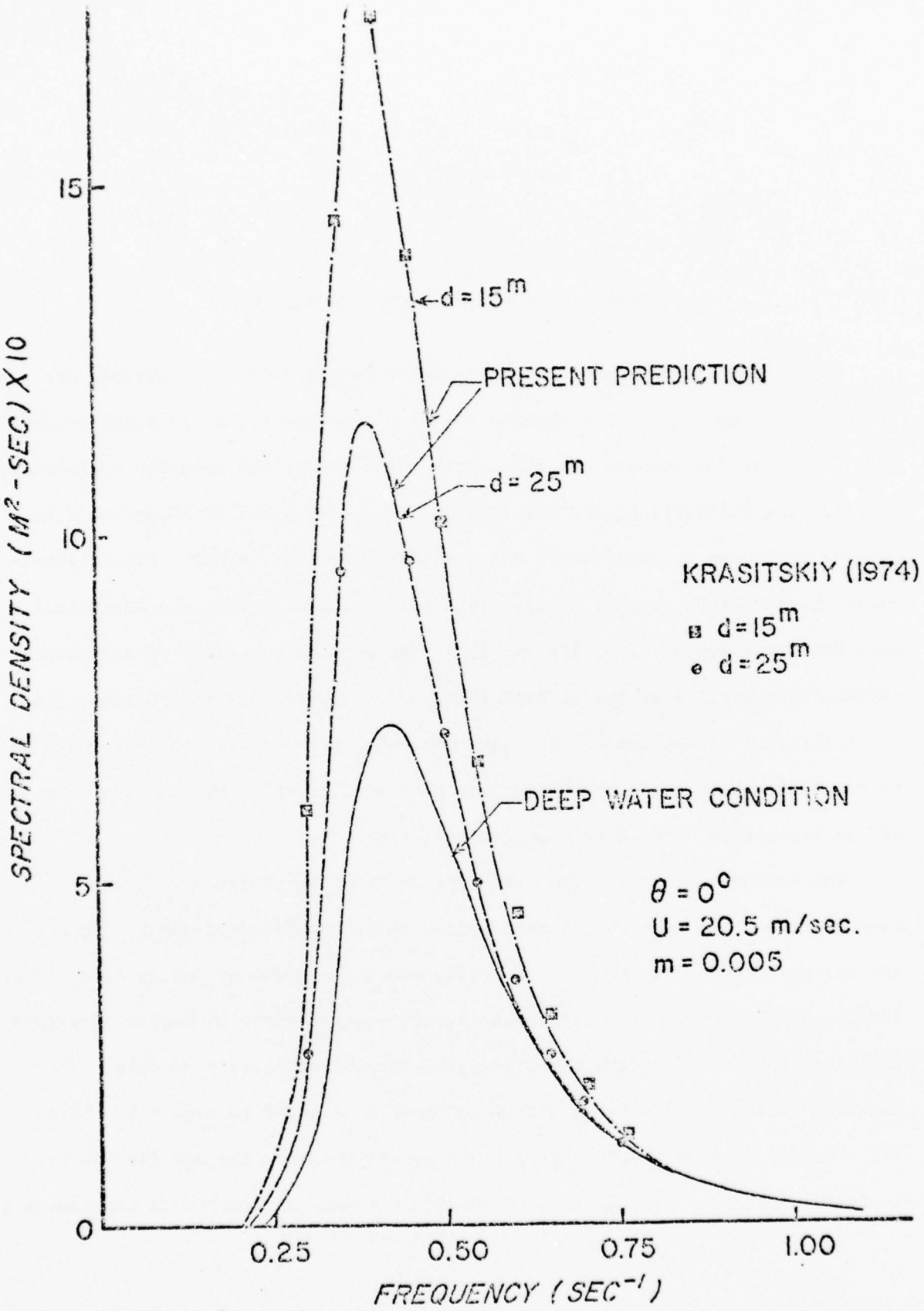

Figure 4 Comparisons of Numerical Results and Analytical Results of Spectrum Transformation Over Parallel Bottom Contour

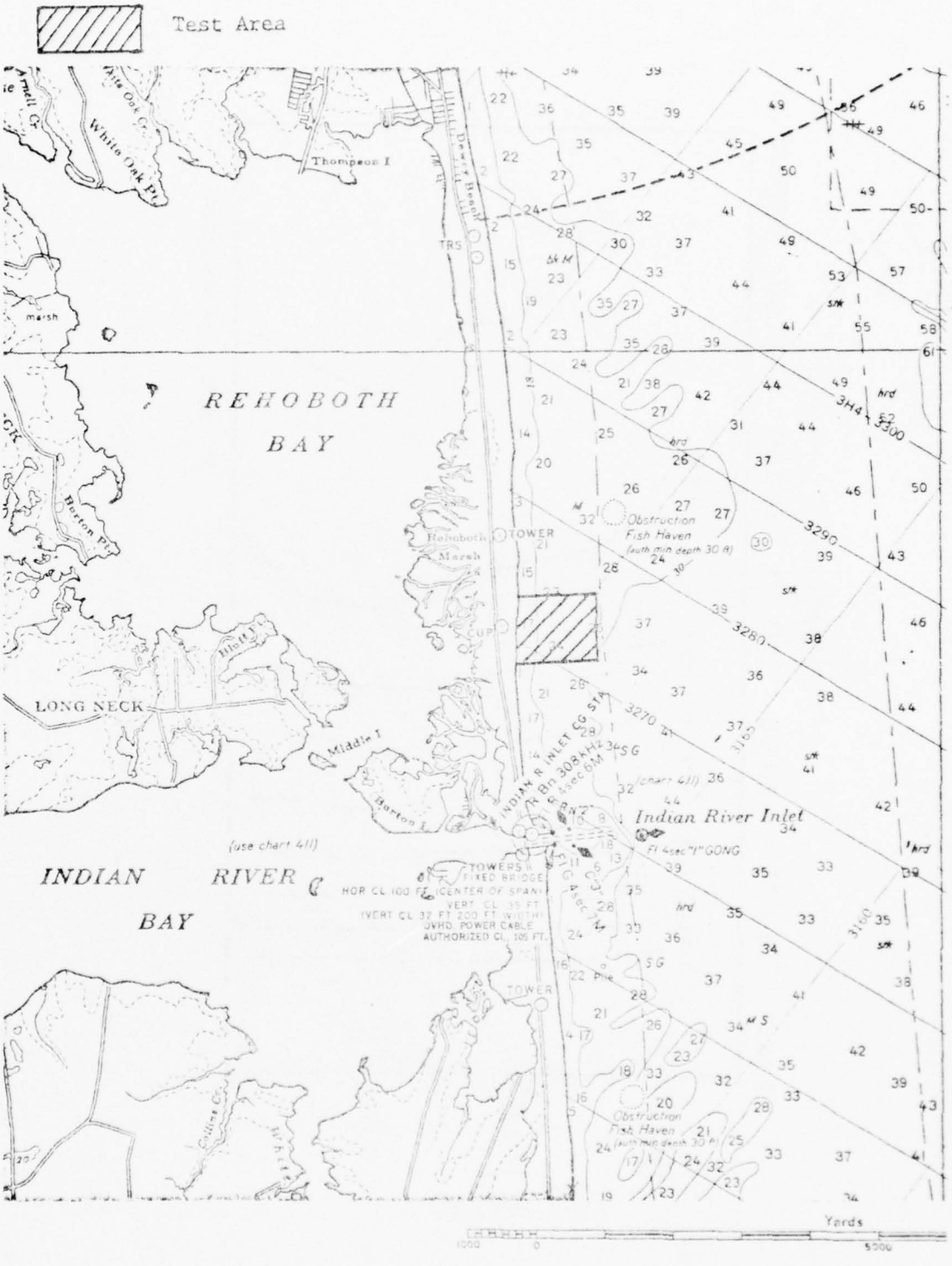

Figure 5 Field Measurement Site, Indian River Inlet, Delaware
(From Map C&GS 1219)

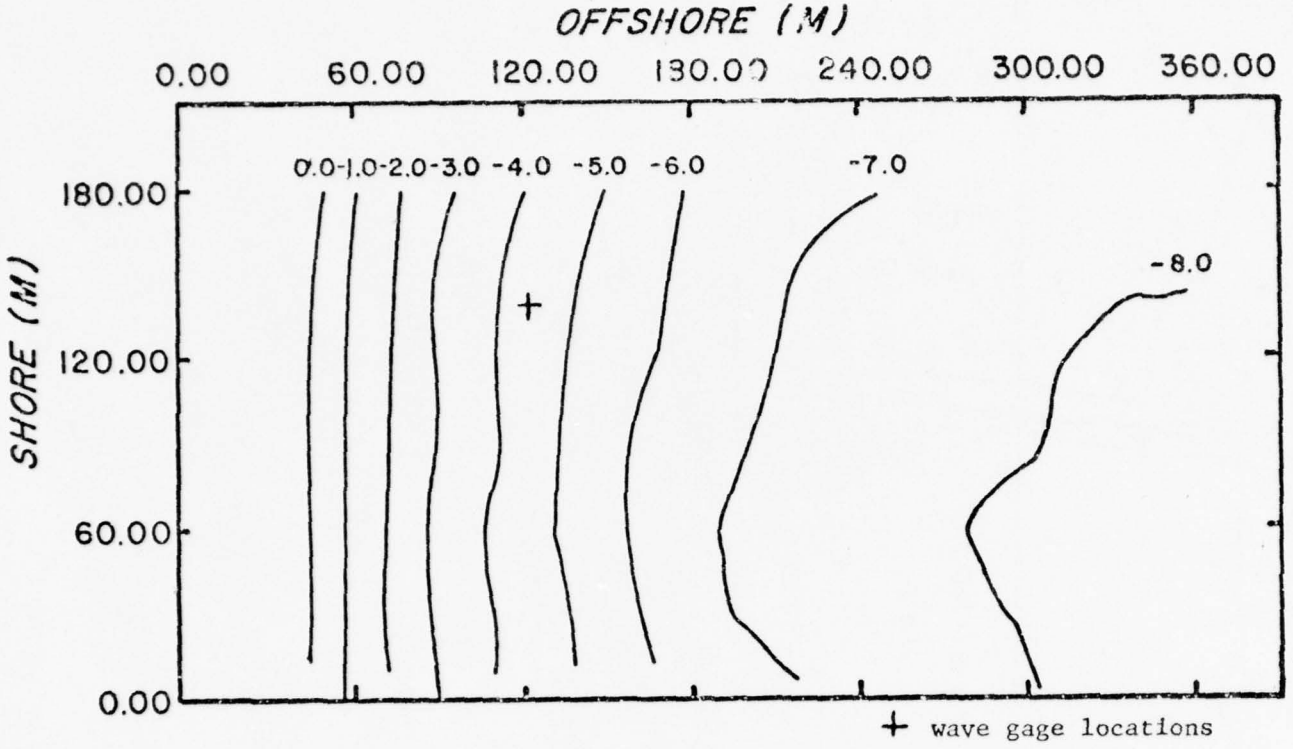

Figure 6 Bottom Profiles and Wave Gage Location

Borchardt (1974) and Hsu (1975). Samples of comparisons are shown in Figure 7. Since there is no simultaneous measurement of deep water wave conditions, the deep water wave spectrum of Pierson-Moskowitz type is again adopted as input condition in the numerical computation. A north-easterly wind of 8.3 m/sec is assumed to prevail. Since the recorded wind speed only indicated a range of 8 - 10 m/sec, the selection of 8.3 m/sec in the computation is merely an estimation. Varying this input wind speed will affect basically the magnitude of the spectral density but hardly the shape of the function.

Finally, the spectrum transformation over a rythmic nearshore hydrograph such as the type described by Sonu (1972) is demonstrated. Assuming that the bathymetry undulates alongshore with diminishing amplitude toward offshore, as shown in Figure 8, such that the water depth, h, in the x-y plane, can be expressed as the superposition of a uniformly sloped beach and a sinusoidal variation:

$$h = -m(x-\Delta x) + A_o\left(1 - \frac{x}{S}\right) \sin \frac{\pi}{2}\left(1 - \frac{y}{\Delta y}\right) + h_o \qquad (20)$$

for $x \leq S$ and

$$h = -m(x-\Delta x) + h_o$$

for $x > S$

where m = beach slope

A_o = amplitude of shoreline undulation

h_o = elevation at origin of coordinate system

S = extent in the offshore direction where bottom undulation begins, beyond which the contour is parallel.

Δx, Δy = grid sizes along the x and y directions respectively.

The values used in the numerical examples are: $m = 0.02$, $A_o = 0.13M$, $h_o = 1M$, $S = 360M$, and $\Delta x = \Delta y = 30M$.

The computed spectral density functions at nodal and anti-nodal points are shown in Figure 9. The results clearly indicate, as expected, that energy flux converges at the convex section of the shoreline and diverges along the concave section.

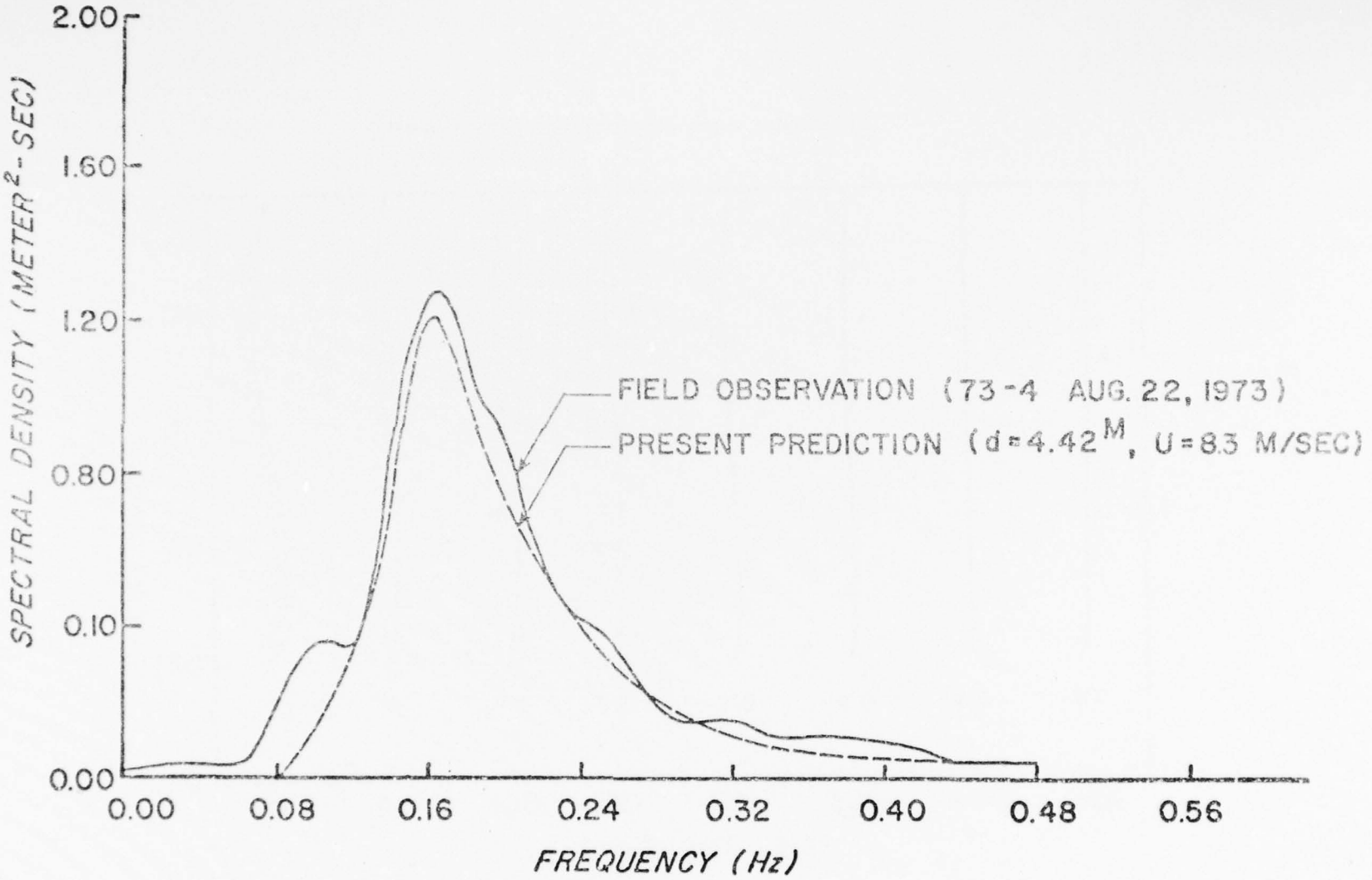

Figure 7 Comparisons of Numerical and Field Results of Spectrum Transformation

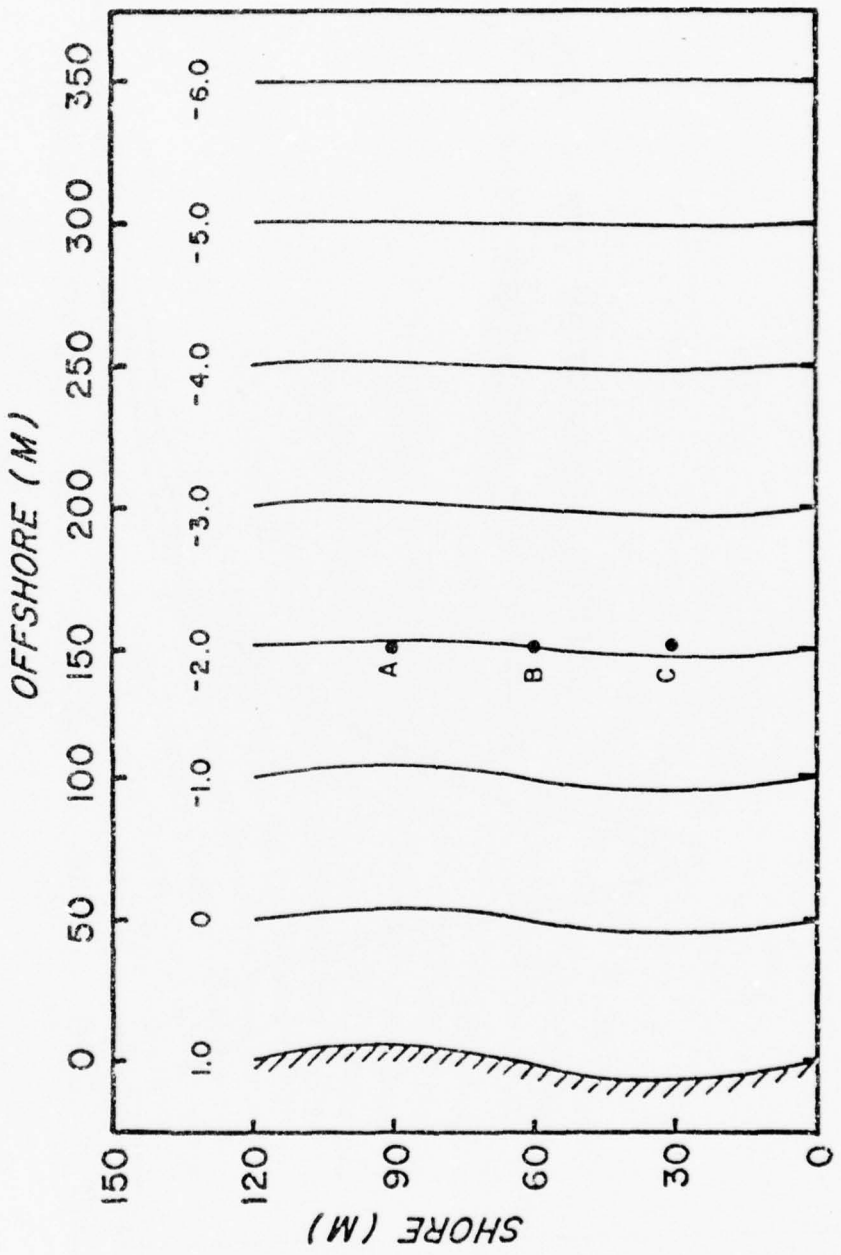

Figure 8 Hypothetical Rhythmic Topography

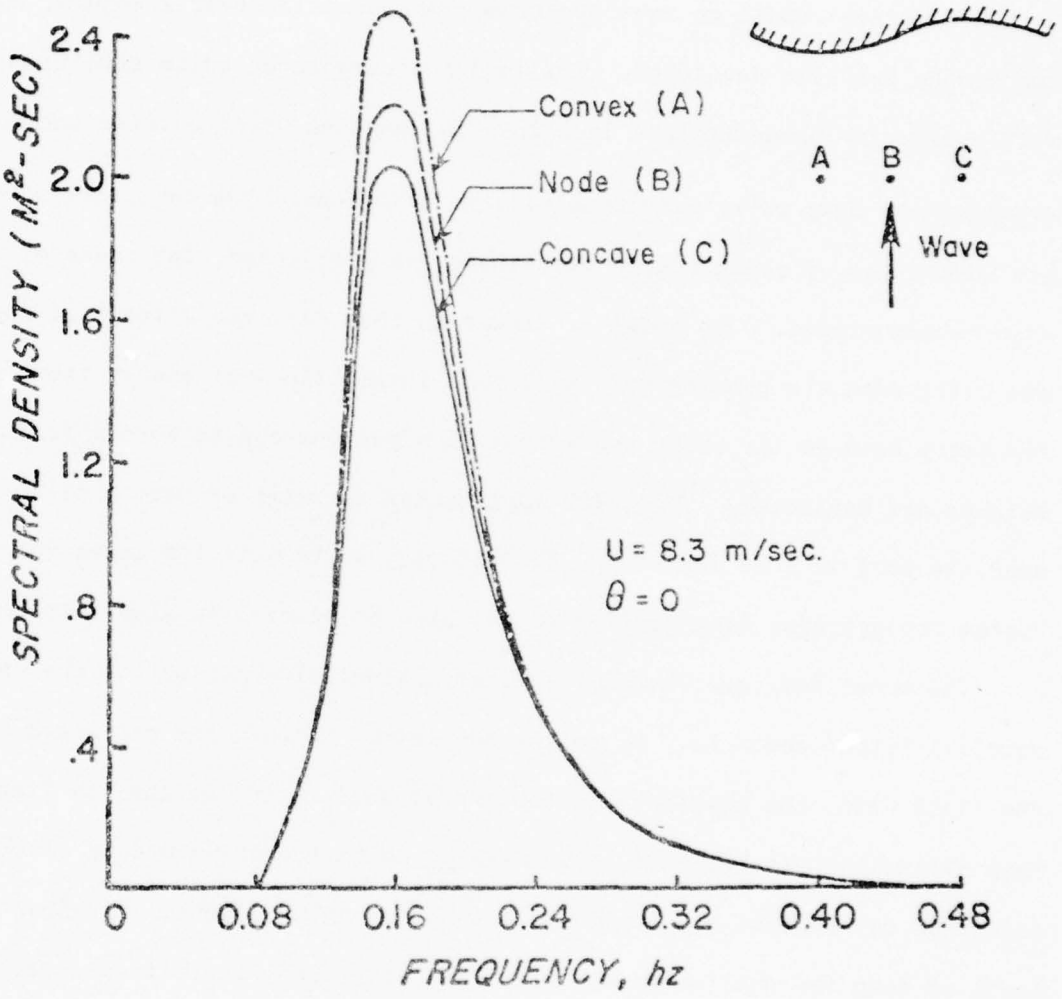

Figure 9 Illustrations of Spatial Variations of Wave Spectrum Over Rhythmic Topography

CHAPTER VI CONCLUSIONS

A numerical model on wave spectrum transformation over irregular bottom topography has been developed. This model proves to be quite effective in predicting wave spectra at predetermined locations in shoaling water outside the surf zone provided the deep water wave condition is specified. The numerical scheme has the advantages of being simple and stable, in particular, for cases of relatively mild bottom slopes. The model is linear in that only the effects of shoaling and refraction are considered. Nonlinear interactions of energy transfer from one frequency band to the other and energy dissipations due to bottom friction and turbulence are neglected. Thus, its application to water of very shallow depth or near the surf line is doubtful. The accuracy of results for cases where the bottom topographies vary rapidly at the side boundaries is also untested.

The model has been verified against analytical solution for the case of parallel bottom contours. As to the comparison between the predicted result and the field data, the agreement is considered good except at the low frequency end. This discrepancy is believed to be mainly due to the assumed deep water input wave condition rather than the nonlinear effects mentioned above. Simultaneous measurements of deep and shallow wave conditions, preferably directional spectrum, should be conducted to establish the field applicability of the model.

It should be noted here that since the present numerical scheme deals with wave height rather than spectral energy density as the basic variables in the governing equations, the incorporation of frictional effects and turbulence energy dissipation is a rather simple matter if such dissipations can be empirically related to the diminishing of wave height. Furthermore, the interactions between waves and currents could also be included as demonstrated by Noda.

References

Borchardt, J., "A Field Study of Measuring the Energy Spectrum of Shallow-Water Ocean Waves," M.S. Thesis, College of Marine Studies, University of Delaware, 1974.

Collins, J. I., "Prediction of Shallow-Water Spectra," J. of Geophys. Res., Vol. 77, No. 15, May, 1972, pp. 2693-2707.

Dette, H.H., "Uber Brandungsstromungen Im Bereich Hoher Reynolds-Zahlen," Heft 41 der Mitteillungen, der Leichtweiss-Instituts fur Wasserbau der Technischen, Universitat Braunschweig, Germany.

Hsu, Y-H. L., "The Photo-Optical Determination of Shallow Water Wave Spectra," M.S. Thesis, College of Marine Studies, University of Delaware, 1975.

Karlsson, T., "Refraction of Continuous Ocean Wave Spectra," J. of Waterways, Harbors and Coastal Eng. Div., ASCE, WW4, Nov. 1969, pp. 437-448.

Krasitskiy, V. P., "Toward a Theory of Transformation of the Spectrum on Refraction of Wind Waves," Izv. Atmospheric and Oceanic Physics, Vol. 10, No. 1, 1974, pp. 72-82.

Lamb, H., Hydrodynamics, 6th Edition, The Macmillan Company, New York, 1932.

LeMehaute, B. and R. C. Y. Koh, "On the Breaking of Waves Arriving at an Angle to the Shore," J. of Hydraulic Res., Vol. 5, No. 1, pp. 67-88, 1967.

Longuet-Higgins, M. S., "On the Transformation of a Continuous Spectrum by Refraction," Proc. Cambridge Phil. Soc., Vol. 53(1), 1957, pp. 226-229.

Longuet-Higgins, M. S., "The Refraction of Sea Waves in Shallow Water," J. F. M., Vol. 1, Part 2, 1956, pp. 163-176.

Noda, E. V., C. J. Sonu, V. C. Rupert and J. I. Collins, "Nearshore Circulations Under Sea Breeze Conditions and Wave-Current Interactions in the Surf Zone," Tetra Tech, Inc., Report TC-149-4, Feb., 1974.

Phillips, O. M., "The Dynamics of the Upper Ocean," Cambridge Univ. Press, 1966.

Pierson, W. J., Jr. and Moskowitz, L., "A Proposed Spectral Form for Fully Developed Wind Seas Based on the Similarity Theory of S. A. Kitaigorodskii," J. of Geophys. Res., Vol. 69, No. 24, Dec., 1964, pp. 5181-5190.

Sonu, C. J., "Field Observations of Nearshore Circulation and Meandering Currents," J. of Geophys. Res., Oceans and Atmospheres, Vol. 77, No. 18, 1972, pp. 3232-3247.

APPENDIX

Computer Flow Chart and

Fortran Listing for Spectrum

Transformation

```
C      A PROGRAM TO COMPUTE SPECTRUM TRANSFORMATION OVER IRREGULAR
C      BOTTOM TOPOGRAPHY
C      GS IS ARRAY OF GRAIN SIZE
C      DW IS ARRAY OF DEPTH OF WATER, XBAR IS ARRAY OF SEA LEVEL INTERCEP
C      MI   = MAX VALUE FOR I SUBSCRIPT, NOT TO EXCEED 100
C      MJ   = MAX VALUE FOR J SUBSCRIPT, NOT TO EXCEED 100
C      TITL = IDENTIFYING TITLE FOR EACH SET.  (12A6).
C      NORAYS = NO. RAYS IN EACH SET.  (I3).
C      T = WAVE PERIOD, SECS,  (F8.2).
C      H = DEEP WATER WAVE HEIGHT,  (F6.2).
C      X,Y = STARTING COORDINATES.  (F7.2).
C      A = INITIAL DIRECTION OF RAY.  (F7.2).
C
       COMMON DW(50,20),U(50,20),V(50,20),Z(50,20),SI(50,20),CO(50,20),
      1H(50,20),CG(50,20),S(50,20),HBREAK(50,20),IB(50,20),DDDX(50,20)
      2,DDDY(50,20),C(50,20)
       COMMON/CON/G,PI,PI2,RAD,EPS,DX,DY,DX2,DY2,T,SIGMA,M,N,IT
       COMMON/STRESS/SIGXY(50,20)
       DIMENSION QSX(100,100),QSY(100,100)
       DIMENSION GS(50,20)
       DIMENSION TITL(12),FMT(2)
       DIMENSION SAVE(50,20)
       COMMON/DTI/DTIS(50)
       COMMON/SPC/H1(20),SIG(20),E0(20),E1(50,20)
       COMMON/DELW/DDW
       INTEGER OPT
97     FORMAT (//' THE ORIGINAL MATRIX OF WATER DEPTH IN METER')
908    FORMAT(//,1X,'TIDAL LEVEL=NN+',F6.2)
98     FORMAT(//,1X,'DX=',F5.2,3X,'DY=',F5.2)
99     FORMAT (/////,1X,'NI=',I5,3X,'NJ=',I5)
100    FORMAT(2I5)
  101  FORMAT(10X,7F10.1/(8F10.1))
  102  FORMAT(3F5.2)
  103  FORMAT(15F 8.3)
C      READ BASIC DATA
       A=135.0
       NT=5.
C        NT=NO. OF DIVISION OF ONE TIDAL CYCLE, NT MUST BE ODD
C       NNT=NO OF TIDAL CYCLES
C      NTS= NO. OF TIME STEPS
       TPER=12.25
       NNT=2
       DT=TPER/FLOAT(NT-1)
        NTS=NT*NNT
       G=9.80621
       PI=3.1415927
       PI2=PI *2.0
       RAD=180.0/PI
       READ (5,100) NI,NJ
C      NI IS NUMBER OF GRID POINTS PERPENDICULAR TO THE SHORE
C      NJ IS THE NUMBER OF GRID POINTS PARALLEL TO THE SHORE
       M=NI
```

```
      N=NJ
      IF(NI.GT.50.OR.NJ.GT.20) GO TO 13
      READ(5,102)DX,DY,AO

      DX2=DX  *2.0
      DY2=DY*2.0
      EPS=0.00005
      NBOUND=5
      JJ=N+2-NBOUND
      NP1=N+1
      READ(5,110)((DW(I,J),J=NBOUND,JJ),I=1,NI)
  110 FORMAT(7F5.1)

      WRITE (6,99) NI,NJ
      WRITE (6,98) DX,DY
      WRITE (6,908) AO
      WRITE (6,97)
      WRITE (6,110) ((DW(I,J),J=NBOUND,JJ),I=1,NI)
      DO 73 I=1,NI
      DO 73 J=NBOUND,JJ
   73 DW(I,J)=DW(I,J)+AO
      DO 151 I=1,NI
      DO 151 J=1,NBOUND-1
  151 DW(I,J)=DW(I,NBOUND)
      DO 150 I=1,NI
      DO 150 J=12,NJ+1

  150 DW(I,J)=DW(I,JJ)
      WRITE (6,108)
      WRITE (6,103) ((DW(I,J),J=1,NP1),I=1,M)
  108 FORMAT (//,1X,'THE AUGMENTED MATRIX OF WATER DEPTH IN METER')

C NBOUND IS THE NO. OF PARALLEL PROFILES BOUNDING THE STUDY AREA ON EACH
      THETAO=A
      THETAO=THETAO/RAD
      THETAO=P12-THETAO
      TIME=0.

      DO 13 K=1,10
      SIG(K)=0.1*PI*FLOAT(K)

      SIGMA=SIG(K)
      T=2.*PI/SIG(K)
      SI4=SIG(K)**4
      SI5=SI4*SIG(K)
      GU=8.3
      CONS=0.74*((9.8/GU)**4)
      AW=0.7779*EXP(-CONS/SI4)/SI5
      EO(K)=0.1945/CONS

      DDW=EO(K)/(AW)
      HO=2.828*SQRT(EO(K))
       DO 141 IT=1,1

      CALL REFRAC(THETAO,HO,IT  ,NBOUND,JJ,K)
  106 CALL LEVEL(NI,NJ,TIME)

  141 CONTINUE
   13 CONTINUE
      STOP
      END
```

```
      SUBROUTINE REFRAC(THETAO,HH,ITER,NBOUND,JJ,K)
      COMMON D (50,20),U(50,20),V(50,20),Z(50,20),SI(50,20),CO(50,20),
     1H(50,20),CG(50,20),S(50,20),HBREAK(50,20),IB(50,20),DDDX(50,20)
     2,DDDY(50,20),C(50,20)
      COMMON/CON/G,PI,PI2,RAD,EPS,DX,DY,DX2,DY2,T,SIGMA,M,N
      COMMON/DTI/DTIS(50)
      COMMON/SPC/H1(20),SIG(20),E0(20),E1(50,20)
      COMMON/DELW/DDW

      M1=M-1
      N1=N+1
      NP1=N+1
      NBM1=NBOUND-1
      N2=N+2
      CALL DEPTH
   10 CALL SNELL(THETAO,HH,NBOUND,JJ)
      CALL ANGLE(20)
      CALL HEIGHT(10,ITER,K)
      RETURN
      END
```

```
      SUBROUTINE DEPTH
      COMMON D (50,20),U(50,20),V(50,20),Z(50,20),SI(50,20),CO(50,20),
     1H(50,20),CG(50,20),W(50,20),HBREAK(50,20),IB(50,20),DDDX(50,20)
     2,DDDY(50,20)
      COMMON/CON/G,PI,PI2,RAD,EPS,DX,DY,DX2,DY2,T,SIGMA,M,N,IT
      MM1=M-1
  156 DO 157 I=2,MM1
      DO 157 J=2,N+1
      A=D(I+1,J)
      IF(A.LT.0.0) A=0.0
      B=D(I-1,J)
      IF(B.LT.0.0) B=0.0
      C=D(I,J+1)
      IF(C.LT.0.0) C=0.0
      E=D(I,J-1)
      IF(E.LT.0.0) E=0.0
      DDDX(I,J)=(A-B)/(2.0*DX)
  157 DDDY(I,J)=(C-E)/(2.0*DY)
      DO 100 J=1,N+1
  100 DDDX(1,J)=DDDX(2,J)
      DO 101 I=1,M
      DDDY(I,1)=DDDY(I,2)
  101 DDDY(I,N+2)=DDDY(I,N+1)
  158 RETURN
      END
```

```
      SUBROUTINE SNELL(THETAO,HH,NBOUND,JJ)
      COMMON D (50,20),U(50,20),V(50,20),Z(50,20),SI(50,20),CO(50,20),
     1H(50,20),CG(50,20),S(50,20),HBREAK(50,20),IB(50,20),DDDX(50,20)
     2,DDDY(50,20)
      COMMON/CON/G,PI,PI2,RAD,EPS,DX,DY,DX2,DY2,T,SIGMA,M,N
      DO 600 J=1,N+2
   30 DO 600 II=1,M
      I=M-II+1
      IF(D(I,J).GT.0.0) GO TO 33
      ANG=PI
      WVHT=0.0
      SS=0.0
      CC=-1.0
      GO TO 43
   33 CONTINUE
      CALL WVNUM(D(I,J),0.0,0.0,0.0,0.0,RK,SIGMA)
      AA=RK*D(I,J)
      ANG=ASIN(SIN(THETAO)*TANH(AA))
      ANG=PI-ANG
      ARG=2.0*AA
      SHOAL=SQRT(1.0/(TANH(AA)*(1.0+ARG/SINH(ARG))))
      REF=SQRT(COS(THETAO)/COS(ANG))
      WVHT=HH*SHOAL*REF
      HB=0.12*TANH(AA)*PI2/RK
      IF(WVHT.GT.HB)WVHT=HB
      IN=1
      IF(WVHT.GT.HB) IN=0
      SS=SIN(ANG)
      CC=COS(ANG)
   43 CONTINUE
      U(I,J)=0.0
      V(I,J)=0.0
      H(I,J)=WVHT
      IB(I,J)=IN
      Z(I,J)=ANG
      SI(I,J)=SS
      CO(I,J)=CC
  600 CONTINUE
  700 RETURN
      END
```

```
 SUBROUTINE GROUP(I,J,DCGDX,DCGDY,FF,RK)
 COMMON D (50,20),U(50,20),V(50,20),Z(50,20),SI(50,20),CO(50,20),
1H(50,20),CG(50,20),S(50,20),HBREAK(50,20),IB(50,20),DDDX(50,20)
2,DDDY(50,20),C3(50,20)
 COMMON/CON/G,PI,PI2,RAD,EPS,DX,DY,DX2,DY2,T,SIGMA,M,N
  DIMENSION DUDX(50,20),DUDY(50,20),DVDX(50,20),DVDY(50,20),
3    DTDY(50,20),DKDX(50,20),DKDY(50,20),E(50,20),DTDX(50,20)
 JJ=J
 DEP=D(I,JJ)
 COSI=CO(I,J)
 SINI=SI(I,J)
 DCGDX=0.0
 DCGDY=0.0
 FF=0.0
 CALL WVNUM(DEP,COSI,SINI,U(I,J),V(I,J),RK,A)
 TA=TANH(RK*DEP)
 HBREAK(I,J)=0.12*PI2*TA/RK
 COSH1=COSH(RK*DEP)
 SECHSQ=1.0/(COSH1**2)
 ARG2=2.0*RK*DEP
 SINH2=SINH(ARG2)
 COSH2=COSH(ARG2)
 SINHSQ=SINH2**2
 E(I,J)=U(I,J)*COSI+V(I,J)*SINI+0.5*A*(1.0+ARG2/SINH2)/RK
 EE=E(I,J)
 C=SQRT(G*TA/RK)
 FF=0.5*(1.0+ARG2/SINH2)
 CG(I,J)=FF*C
 DUDX(I,J)=(U(I+1,J)-U(I-1,J))/DX2
 DUDY(I,J)=(U(I,J+1)-U(I,J-1))/DY2
 DVDX(I,J)=(V(I+1,J)-V(I-1,J))/DX2
 DVDY(I,J)=(V(I,J+1)-V(I,J-1))/DY2
 DTDX(I,J)=(Z(I+1,J)-Z(I-1,J))/DX2
 DTDY(I,J)=(Z(I,J+1)-Z(I,J-1))/DY2
 DKDX(I,J)=RK*((U(I,J)*SINI-V(I,J)*COSI)*DTDX(I,J)-(COSI*DUDX(I,J)+
1SINI*DVDX(I,J))-A*DDDX(I,J  )/SINH2)/EE
 DKDY(I,J)=RK*((U(I,J)*SINI-V(I,J)*COSI)*DTDY(I,J) -(COSI*DUDY(I,J)
1 +SINI*DVDY(I,J))-A*DDDY(I,J  )/SINH2)/EE
 P=C*(SINH2-ARG2*COSH2)/SINHSQ
 DKDDX=RK*DDDX(I,JJ)+DEP*DKDX(I,J)
 DKDDY=RK*DDDY(I,JJ)+DEP*DKDY(I,J)
 Q=0.5*G/(C*RK**2)
   C3(I,J)=C
 DCDX=Q*(RK*SECHSQ*DKDDX-TA*DKDX(I,J))
 DCDY=Q*(RK*SECHSQ*DKDDY-TA*DKDY(I,J))
 DCGDX=P*DKDDX+FF*DCDX
 DCGDY=P*DKDDY+FF*DCDY
 RETURN
 END
```

```
      SUBROUTINE LEVEL(NI,NJ,TIME)
      COMMON D(50,20),U(50,20),V(50,20),Z(50,20),SI(50,20),CO(50,20),
     1H(50,20),CG(50,20),S(50,20),HBREAK(50,20),IB(50,20),DDDX(50,20)
     2,DDDY(50,20),C(50,20)
      COMMON/CON/G,PI,PI2,RAD,EPS,DX,DY,DX2,DY2,T,SIGMA,M,N
      DIMENSION XBAR(20)
C     LINEAR INTERPOLATION OF SEA LEVEL POSITION

  111 FORMAT('NO SEA LEVEL INTERCEPT ALONG LINE', I5)
  104  FORMAT(7F6.2)
       REAL INCREX

      DO 2 J=1,NJ
      DO 3 I=1,NI
      IF(D(I,J).GT.0.) GO TO 4
    3 CONTINUE
      WRITE(6,111)J
       GO TO 2
    4 INCREX=-DX*D(I,J)/(D(I-1,J)-D(I,J))
              XBAR(J)=FLOAT(I)*DX-DX/2.-INCREX
    2 CONTINUE
      RETURN
      END
```

```
      SUBROUTINE NEWHT(I,J,IFLAG)
      COMMON D(50,20),U(50,20),V(50,20),Z(50,20),SI(50,20),CO(50,20),
     1H(50,20),CG(50,20),S(50,20),HBREAK(50,20),IB(50,20),DDDX(50,20)
     2,DDDY(50,20)
      COMMON/CON/G,PI,PI2,RAD,EPS,DX,DY,DX2,DY2,T,SIGMA,M,N
      COMMON/XBR/XBREAK(20),SAVE(50,20)
      SAVE(M,J)=H(M,J)
      IB(I,J)=1
      N1=N+1
      N2=N+2
      CC1=(V(I,J)+CG(I,J)*SI(I,J))/DY
      CC2=(U(I,J)+CG(I,J)*CO(I,J))/DX
      HNEW= (CC1*H(I,J-1)-CC2*H(I+1,J))/(CC1-CC2-S(I,J)/2.0)
       IF(HNEW. LT. 0.0) HNEW=0.0
      SAVE(I,J)=HNEW
      IF(HNEW.LE.HBREAK(I,J)) GO TO 850
    3 HNEW=HBREAK(I,J)
      IB(I,J)=0
  850 CONTINUE
  860 IF(ABS(HNEW-H(I,J)).GT.(EPS*ABS(HNEW))) IFLAG=0
      H(I,J)=HNEW
  899 RETURN
      END
```

```
      SUBROUTINE HEIGHT(ITMAX,KK,K)
      COMMON D (50,20),U(50,20),V(50,20),Z(50,20),SI(50,20),CO(50,20),
     1H(50,20),CG(50,20),S(50,20),HBREAK(50,20),IB(50,20),DDDX(50,20)
     2,DDDY(50,20),C(50,20)
      COMMON/CON/G,PI,PI2,RAD,EPS,DX,DY,DX2,DY2,T,SIGMA,M,N
      COMMON/STRESS/SIGXY(50,20)
      COMMON/XBR/XBREAK(20),SAVE(50,20)
      COMMON/CCIJ/CC(50,20)
      COMMON/SPC/H1(20),SIG(20),E0(20),E1(50,20)
      COMMON/DELW/DDW
      DIMENSION AAW(50,20)
       DIMENSION AZ(50,20)
      COMMON/DTI/DTIS(50)
      M1=M-1

      N1=N+1
C     COMEPUTE VALUES OF S(I,J)
      DO 500 I=2,M1
      DO 500 J=2,N1
      IF(D(I,J).LE.0.0) GO TO 500
      CALL GROUP(I,J,DCGDX,DCGDY,FF,RK)
      DUDX=(U(I+1,J)-U(I-1,J))/DX2
      DUDY=(U(I,J+1)-U(I,J-1))/DY2
      DVDX=(V(I+1,J)-V(I-1,J))/DX2
      DVDY=(V(I,J+1)-V(I,J-1))/DY2
      DTDX=(Z(I+1,J)-Z(I-1,J))/DX2
      DTDY=(Z(I,J+1)-Z(I,J-1))/DY2
      SS2=SI(I,J)**2
      CC2=CO(I,J)**2
      SIGXX=(2.0*FF-0.5)*CC2+(FF-0.5)*SS2
      SIGYY=(2.0*FF-0.5)*SS2+(FF-0.5)*CC2
      TAUXY=FF*SI(I,J)*CO(I,J)
      SIGXY(I,J)=TAUXY
      S(I,J)=CG(I,J)*(SI(I,J)*DTDX-CO(I,J)*DTDY)-(DUDX+DVDY)-(CO(I,J)*DC
     1GDX+SI(I,J)*DCGDY)-(SIGXX*DUDX+TAUXY*DUDY+TAUXY*DVDX+SIGYY*DVDY)
  500 CONTINUE
      N2=N+2
      M2=M-2
      DO 510 II=1,M2
      I=M-II
      DO 580 IT=1,ITMAX
      IFLAG=1
      DO 520 J=2,N1
      IF(D(I,J).LE.0.0) GO TO 520
      CALL NEWHT(I,J,IFLAG)
  520 CONTINUE
      IF(IFLAG.EQ.1) GO TO 570
  580 CONTINUE
      WRITE(6,540) I,IT
  540 FORMAT(' RELAXATION FOR THE WAVE HEIGHT FAILED TO CONVERGE',
     1'ON ROE',I5,'AFTER',I6,'ITERATIONS')
      WRITE(6,541)(H(I,J),J=1,N2   )
  541 FORMAT('  LAST VALUES OF H ARE'/,(10F13.5)  )
      RETURN
  570 WRITE(6,542) I,IT
  542 FORMAT(10X,' RELAXATION FOR WAVE HEIGHT CONVERGED ON ROW',I6,3X,'A
     1FTER',I6,'ITERATIONS')
  510 CONTINUE
```

```
      WRITE (6,6052)
 6052 FORMAT (//,1X,'WAVE HEIGHT MATRIX'/)
      WRITE(6,652)((H(I,J),J=1,N1),I=1,M)
      WRITE(6,6053)
 6053 FORMAT (//,1X,'BREAKING POSITION ("0"MEANS WAVE BREAKING)')
      WRITE(6,653)((IB(I,J),J=1,N1),I=1,M)
  653 FORMAT(1518)
  652 FORMAT(15F8.3)
      DO 575 J=1,N1
      A=0.
      DO 560 II=1,M2

      I=M-II
        IF(A.GT.0.) GO TO 575
      DXX=0.
      DDXX=HBREAK(I+1,J)-HBREAK(I,J)
      IF(SAVE(I,J)-HBREAK(I,J))560,560,554
  554 DDX=((SAVE(I,J)-HBREAK(I,J))/(SAVE(I,J)-SAVE(I+1,J)+DDXX))*DX

  557 XBREAK(J)=FLOAT(I)*DX-DX/2.+DDX+DXX
       A=XBREAK(J)
      GO TO 560
  555 DDX=0.
      XBREAK(J)=FLOAT(I)*DX-DX/2.+DDX+DXX
        A=XBREAK(J)
  560 CONTINUE
  575 CONTINUE
      NBOUND=5
      NB=NBOUND
      JJ=11
      DO 702 I=1,M
      DO 702 J=NB,JJ
      E1(I,J)=H(I,J)**2/8.
  702 AAW(I,J)=E1(I,J)/(DDW)
      WRITE (6,112) SIGMA
  112 FORMAT (//,1X,'OFFSHORE ENERGY DENSITY AT SIGMA=',F8.3)
      WRITE (6,113) E0(K),AW
  113 FORMAT (10X,'E0(K)=',F10.3,10X,'AW=',F10.3)
      WRITE(6,704)SIGMA
  704 FORMAT(//,1X,'NEARSHORE ENERGY DENSITY AT SIGMA=',F8.3)
      WRITE(6,651)((AAW(I,J),J=NB,JJ),I=1,M)
  651 FORMAT(7F10.4)

      WRITE (6,6051) SIGMA
 6051 FORMAT (//,1X,'END OF CALCULATION AT SIGMA=',F8.3,/,
     1' ***   ***   ***   ***   ***   ***   ***   ***   ***   ***')
      RETURN
      END
```

```
      SUBROUTINE ANGLE(ITMAX)
      COMMON D (50,20),U(50,20),V(50,20),Z(50,20),SI(50,20),CO(50,20),
     1H(50,20),CG(50,20),S(50,20),HBREAK(50,20),IB(50,20),DDDX(50,20)
     2,DDDY(50,20)
      COMMON/CON/G,PI,PI2,RAD,EPS,DX,DY,DX2,DY2,T,SIGMA,M,N
      N1=N+1
       N2=N+2
      M1=M-1
      M2=M-2
      DO 200 IT=1,ITMAX
      IFLAG=1
      DO 210 J=2,N1
      DO 211 II=2,M1
      I=M-II+1
      IF(D(I,J).LE.0.0.OR.D(I-1,J).LE.0.0) GO TO 211
      CALL NEWANG(I,J,IFLAG,2)
  211 CONTINUE
  210 CONTINUE
      IF(IFLAG.EQ.1) GO TO 250
  200 CONTINUE
      WRITE(6,220) ITMAX
  220 FORMAT(' RELAXATION FOR THETA FAILED AFTER',I6,3X,'ITERATIONS')
  250 WRITE(6,251) I,IT
  251 FORMAT(10X,' RELAXATION FOR    THETA    CONVERGED ON ROW',I6,3X,'A
     1FTER',I6,' ITERATIONS')
      WRITE (6,2501)
 2501 FORMAT (//,1X,'WAVE APPROACHING ANGLE IN RADIAN')
      WRITE(6,252)((Z(I,J),J=1,N1),I=1,M)
  252 FORMAT(15F8.3)
            RETURN
      END
```

```
      SUBROUTINE NEWANG(I,J,IFLAG,IM)
      COMMON D (50,20),U(50,20),V(50,20),Z(50,20),SI(50,20),CO(50,20),
     1H(50,20),CG(50,20),S(50,20),HBREAK(50,20),IB(50,20),DDDX(50,20)
     2,DDDY(50,20)
      COMMON/CON/G,PI,PI2,RAD,EPS,DX,DY,DX2,DY2,T,SIGMA,M,N
C STATEMENT FUNCTIONS
      DUDX(I,J)=(U(I+1,J)-U(I-1,J))/DX2
      DUDY(I,J)=(U(I,J+1)-U(I,J-1))/DY2
      DVDX(I,J)=(V(I+1,J)-V(I-1,J))/DX2
      DVDY(I,J)=(V(I,J+1)-V(I,J-1))/DY2
      F(I,J)=U(I,J)*COSI+V(I,J)*SINI + 0.5*A*(1.0 + ARG2/SINH2)/RK
      DKDY(I,J)=(-(COSI*DUDY(I,J) + SINI*DVDY(I,J))-A*DDDY(I,J  )/SINH2
     1/FF
      DKDX(I,J)=(-(COSI*DUDX(I,J)+SINI*DVDX(I,J))-A*DDDX(I,J  )/SINH2)/
     1F
      FAC(I,J)=U(I,J)*SINI-V(I,J)*COSI
      COSI=CO(I,J)
       SINI=SI(I,J)
      JJ=J
      CALL WVNUM(D(I,JJ),COSI,SINI,U(I,J),V(I,J),RK,A)
      ARG2=2.0*RK*D(I,JJ)
      SINH2=SINH(ARG2)
      FF=F(I,J)
      IF(FF.GT.0.0) GO TO 450
      WRITE(6,451) I,J,D(I,JJ),COSI,SINI,U(I,J),V(I,J),RK,A
  451 FORMAT(10X,'FF IS NEGATIVE--OUTPUT I,J,D,COSI,SINI,U,V,RK,A'/,
     1215,7E13.4)
      RETURN
  450 FACI=FAC(I,J)
      DEN1=(SINI-COSI*FACI/FF)/DY
      DEN2=(COSI+SINI*FACI/FF)/DX
      DEN=DEN1-DEN2
      ZNEW=(COSI*DKDY(I,J)-SINI*DKDX(I,J)+Z(I,J-1)*DEN1-Z(I+1,J)*DEN2)/
     1EN
      IF(ABS(ZNEW-Z(I,J)).GT.(EPS*ABS(ZNEW))) IFLAG=0
      Z(I,J)=ZNEW
      CO(I,J)=COS(Z(I,J))
      SI(I,J)=SIN(Z(I,J))
       RETURN
      END
```

```
      SUBROUTINE WVNUM(D,COSI,SINI,U,V,RK,A)
C SUBROUTINE COMPUTES THE WAVE NUMBER INCLUDING WAVE-CURRENT INTERATION
      COMMON/CON/G,PI,PI2,RAD,EPS,DX,DY,DX2,DY2,T,SIGMA,M,N

      EPSK=0.0005
      RK=PI2/(T*SQRT(G*D))
      DO 100 I=1,50
      A=SIGMA-U*RK*COSI-V*RK*SINI
      A2=A**2
      ARG=RK*D
      F1=EXP(ARG)
      F2=1.0/F1
      SECH=2.0/(F1+F2)
      SECH2=SECH*SECH
      TT=TANH (ARG)
      FK=G*RK*TT-A2
      FFK=G*(ARG*SECH2+TT)+2.0*(U*COSI+V*SINI)*A
      RKNEW=RK-FK/FFK
      IF(ABS(RKNEW-RK).LE.(ABS(EPSK*RKNEW))) GO TO 110
      RK=RKNEW
  100 CONTINUE
      WRITE(6,101) I,RK,T,D,U,V
  101 FORMAT('  ITERATION FOR K FAILED TO CONVERGE AFTER',I6,3X,5F10.4)
      RETURN
  110 RK=RKNEW
      A=SIGMA-U*RK*COSI-V*RK*SINI
      IF(RK.GT.0.0) GO TO 120
            WRITE(6,130) D,COSI,SINI,U,V,RK,A
  130 FORMAT(10X,'RK IS NEGATIVE--OUTPUT D,COSI,SINI,U,V,RK,A'/,7E12.4)
  120 RETURN
      END
```

NI= 13 NJ= 14

DX=10.00 DY=20.00

TIDAL LEVEL=NN+ 0.35

THE ORIGINAL MATRIX OF WATER DEPTH IN METER

-0.8	-0.8	-0.6	-0.6	-0.5	-0.4	-0.4
-0.3	-0.4	-0.4	-0.4	-0.3	-0.2	-0.1
-0.2	-0.2	-0.2	-0.2	0.0	0.0	0.0
0.0	0.4	0.3	0.5	0.5	0.6	0.7
0.6	0.8	1.0	1.1	1.1	1.1	1.2
1.1	1.5	1.5	1.8	1.8	1.6	1.7
1.8	2.0	2.2	2.2	2.0	2.5	2.3
2.5	2.5	2.6	2.6	2.7	2.8	3.0
3.0	3.0	3.2	3.0	3.5	3.6	3.5
3.4	3.5	3.5	3.5	4.0	4.0	4.0
3.5	3.8	3.8	3.8	4.2	4.1	4.2
3.6	3.9	3.9	4.0	4.5	4.3	4.3
3.8	4.0	4.0	4.3	4.6	4.4	4.4

THE AUGMENTED MATRIX OF WATER DEPTH IN METER

-0.450	-0.450	-0.450	-0.450	-0.450	-0.450	-0.250	-0.250	-0.150	-0.050	-0.050	-0.050	-0.050
0.050	0.050	0.050	0.050	0.050	-0.050	-0.050	-0.050	0.050	0.150	0.250	0.250	0.250
0.150	0.150	0.150	0.150	0.150	0.150	0.150	0.150	0.350	0.350	0.350	0.350	0.350
0.350	0.350	0.350	0.350	0.350	0.750	0.650	0.850	0.850	0.950	1.050	1.050	1.050
0.950	0.950	0.950	0.950	0.950	1.150	1.350	1.450	1.450	1.450	1.550	1.550	1.550
1.450	1.450	1.450	1.450	1.450	1.850	1.850	2.150	2.150	1.950	2.050	2.050	2.050
2.150	2.150	2.150	2.150	2.150	2.350	2.550	2.550	2.350	2.850	2.650	2.650	2.650
2.850	2.850	2.850	2.850	2.850	2.850	2.950	2.950	3.050	3.150	3.350	3.350	3.350
3.350	3.350	3.350	3.350	3.350	3.350	3.550	3.350	3.850	3.950	3.850	3.850	3.850
3.750	3.750	3.750	3.750	3.750	3.850	3.850	3.850	4.350	4.350	4.350	4.350	4.350
3.850	3.850	3.850	3.850	3.850	4.150	4.150	4.150	4.550	4.450	4.550	4.550	4.550
3.950	3.950	3.950	3.950	3.950	4.250	4.250	4.350	4.850	4.650	4.650	4.650	4.650
4.150	4.150	4.150	4.150	4.150	4.350	4.350	4.650	4.950	4.750	4.750	4.750	4.750

WAVE APPROACHING ANGLE IN RADIAN

3.142	3.142	3.142	3.142	3.142	3.142	3.142	3.142	3.142	3.142	3.142	3.142	3.142
3.157	3.157	3.157	3.157	3.157	3.142	3.142	3.142	3.157	3.169	3.177	3.177	3.177
3.169	3.168	3.169	3.169	3.268	3.169	3.169	3.169	3.246	3.197	3.195	3.182	3.184
3.184	3.182	3.182	3.182	3.325	3.297	3.231	3.272	3.231	3.230	3.226	3.205	3.207
3.211	3.204	3.205	3.205	3.275	3.301	3.256	3.290	3.247	3.229	3.238	3.224	3.226
3.227	3.223	3.223	3.223	3.283	3.294	3.257	3.312	3.272	3.236	3.245	3.238	3.240
3.245	3.240	3.240	3.240	3.273	3.291	3.257	3.312	3.300	3.261	3.253	3.251	3.253
3.261	3.256	3.256	3.256	3.281	3.284	3.262	3.330	3.301	3.263	3.276	3.264	3.266
3.271	3.268	3.268	3.268	3.294	3.292	3.269	3.333	3.314	3.264	3.280	3.276	3.277
3.279	3.277	3.277	3.277	3.302	3.296	3.279	3.328	3.311	3.277	3.291	3.285	3.286
3.280	3.281	3.281	3.281	3.302	3.301	3.285	3.317	3.305	3.283	3.296	3.291	3.292
3.282	3.283	3.283	3.283	3.293	3.296	3.290	3.308	3.303	3.287	3.295	3.294	3.294
3.286	3.286	3.286	3.286	3.286	3.289	3.289	3.294	3.299	3.296	3.296	3.296	3.296

OFFSHORE ENERGY DENSITY AT SIGMA= 0.314
EO(K)= 0.135 AW= 0.000

NEARSHORE ENERGY DENSITY AT SIGMA= 0.314

0.0000	0.0000	0.0000	0.0000	0.0000	0.0000	0.0000
0.0000	0.0000	0.0000	0.0000	0.0000	0.0000	0.0000
0.0000	0.0000	0.0000	0.0000	0.0000	0.0000	0.0000
0.0000	0.0000	0.0000	0.0000	0.0000	0.0000	0.0000
0.0000	0.0000	0.0000	0.0000	0.0000	0.0000	0.0000
0.0000	0.0000	0.0000	0.0000	0.0000	0.0000	0.0000
0.0000	0.0000	0.0000	0.0000	0.0000	0.0000	0.0000
0.0000	0.0000	0.0000	0.0000	0.0000	0.0000	0.0000
0.0000	0.0000	0.0000	0.0000	0.0000	0.0000	0.0000
0.0000	0.0000	0.0000	0.0000	0.0000	0.0000	0.0000
0.0000	0.0000	0.0000	0.0000	0.0000	0.0000	0.0000
0.0000	0.0000	0.0000	0.0000	0.0000	0.0000	0.0000
0.0000	0.0000	0.0000	0.0000	0.0000	0.0000	0.0000

NEARSHORE ENERGY DENSITY AT SIGMA= 0.628

0.0000	0.0000	0.0000	0.0000	0.0000	0.0000	0.0000
0.0000	0.0000	0.0000	0.0000	0.0000	0.0000	0.0000
0.0000	0.0000	0.0000	0.0000	0.0000	0.0000	0.0000
0.0000	0.0002	0.0002	0.0003	0.0003	0.0004	0.0004
0.0004	0.0005	0.0007	0.0008	0.0008	0.0008	0.0009
0.0008	0.0011	0.0013	0.0011	0.0008	0.0013	0.0011
0.0011	0.0009	0.0011	0.0010	0.0008	0.0010	0.0010
0.0010	0.0009	0.0010	0.0010	0.0007	0.0009	0.0009
0.0009	0.0008	0.0009	0.0009	0.0007	0.0008	0.0008
0.0008	0.0008	0.0008	0.0008	0.0007	0.0008	0.0008
0.0008	0.0008	0.0008	0.0008	0.0007	0.0007	0.0007
0.0008	0.0008	0.0008	0.0008	0.0007	0.0007	0.0007
0.0008	0.0008	0.0008	0.0007	0.0007	0.0007	0.0007

NEARSHORE ENERGY DENSITY AT SIGMA= 0.942

0.0000	0.0000	0.0000	0.0000	0.0000	0.0000	0.0000
0.0002	0.0000	0.0000	0.0000	0.0002	0.0020	0.0055
0.0020	0.0020	0.0020	0.0020	0.0107	0.0107	0.0107
0.0107	0.0477	0.0361	0.0609	0.0609	0.0756	0.0918
0.0756	0.1095	0.1490	0.1705	0.0899	0.1709	0.0970
0.1709	0.1417	0.2713	0.1413	0.0836	0.2996	0.0960
0.1783	0.1291	0.2142	0.1594	0.0885	0.2292	0.1137
0.1556	0.1276	0.1762	0.1642	0.0959	0.1818	0.1249
0.1454	0.1265	0.1524	0.1584	0.1030	0.1511	0.1304
0.1395	0.1263	0.1390	0.1469	0.1124	0.1346	0.1303
0.1357	0.1272	0.1320	0.1371	0.1200	0.1286	0.1287
0.1325	0.1282	0.1290	0.1310	0.1237	0.1261	0.1270
0.1291	0.1278	0.1278	0.1261	0.1247	0.1256	0.1256

NEARSHORE ENERGY DENSITY AT SIGMA= 1.257

0.0000	0.0000	0.0000	0.0000	0.0000	0.0000	0.0000
0.0002	0.0000	0.0000	0.0000	0.0002	0.0016	0.0045
0.0016	0.0016	0.0016	0.0000	0.0086	0.0086	0.0086
0.0086	0.0380	0.0288	0.0000	0.0483	0.0596	0.0000
0.0596	0.0855	0.1152	0.0006	0.0986	0.0000	0.0000
0.1314	0.0735	0.2044	0.0211	0.0427	0.2245	0.0000
0.1150	0.0766	0.2187	0.0653	0.0395	0.4066	0.0000
0.1077	0.0809	0.1610	0.1135	0.0424	0.2633	0.0211
0.1061	0.0856	0.1250	0.1316	0.0539	0.1620	0.0648
0.1051	0.0908	0.1083	0.1192	0.0729	0.1198	0.0909
0.1035	0.0958	0.1011	0.1095	0.0882	0.1039	0.0997
0.1012	0.0987	0.0991	0.1030	0.0964	0.0990	0.1002
0.0989	0.0989	0.0989	0.0990	0.0992	0.0990	0.0990

NEARSHORE ENERGY DENSITY AT SIGMA= 1.571

0.0000	0.0000	0.0000	0.0000	0.0000	0.0000	0.0000
0.0001	0.0000	0.0000	0.0000	0.0000	0.0000	0.0000
0.0007	0.0007	0.0000	0.0000	0.0000	0.0000	0.0000
0.0039	0.0167	0.0000	0.0000	0.0000	0.0000	0.0000
0.0259	0.0366	0.0007	0.0000	0.0000	0.0000	0.0000
0.0267	0.0576	0.0000	0.0000	0.0014	0.0000	0.0000
0.0297	0.0463	0.1393	0.0092	0.0031	0.0000	0.0006
0.0364	0.0409	0.1729	0.0044	0.0000	0.0000	0.0046
0.0428	0.0402	0.0666	0.0000	0.0425	0.0000	0.0028
0.0468	0.0424	0.0513	0.0905	0.0157	0.1304	0.0287
0.0482	0.0456	0.0475	0.0573	0.0368	0.0590	0.0413
0.0478	0.0475	0.0471	0.0508	0.0461	0.0493	0.0485
0.0472	0.0476	0.0476	0.0483	0.0491	0.0486	0.0486

NEARSHORE ENERGY DENSITY AT SIGMA= 1.885

0.0000	0.0000	0.0000	0.0000	0.0000	0.0000	0.0000
0.0000	0.0000	0.0000	0.0000	0.0000	0.0000	0.0000
0.0000	0.0003	0.0000	0.0000	0.0000	0.0000	0.0000
0.0000	0.0072	0.0000	0.0000	0.0000	0.0000	0.0000
0.0000	0.0152	0.0000	0.0000	0.0000	0.0000	0.0000
0.0000	0.0326	0.0000	0.0000	0.0000	0.0000	0.0000
0.0005	0.0458	0.0510	0.0000	0.0000	0.0000	0.0000
0.0054	0.0586	0.0193	0.0000	0.0000	0.0000	0.0000
0.0128	0.0343	0.0187	0.0015	0.0000	0.0000	0.0000
0.0193	0.0258	0.0206	0.0803	0.0000	0.0000	0.0000
0.0226	0.0240	0.0219	0.0382	0.0117	0.0146	0.0546
0.0234	0.0240	0.0232	0.0261	0.0224	0.0263	0.0229
0.0235	0.0239	0.0239	0.0244	0.0249	0.0246	0.0246

NEARSHORE ENERGY DENSITY AT SIGMA= 2.199

0.0000	0.0000	0.0000	0.0000	0.0000	0.0000	0.0000
0.0000	0.0000	0.0000	0.0000	0.0000	0.0000	0.0000
0.0000	0.0000	0.0000	0.0000	0.0000	0.0000	0.0000
0.0000	0.0000	0.0000	0.0000	0.0000	0.0000	0.0000
0.0000	0.0000	0.0000	0.0000	0.0000	0.0000	0.0000
0.0000	0.0000	0.0000	0.0000	0.0000	0.0000	0.0000
0.0000	0.0000	0.0000	0.0000	0.0000	0.0000	0.0000
0.0005	0.0213	0.0000	0.0000	0.0003	0.0000	0.0000
0.0041	0.0242	0.0011	0.0000	0.0005	0.0000	0.0000
0.0088	0.0186	0.0059	0.0263	0.0007	0.0000	0.0000
0.0116	0.0140	0.0105	0.0209	0.0056	0.0281	0.0026
0.0125	0.0131	0.0123	0.0140	0.0119	0.0147	0.0113
0.0127	0.0128	0.0128	0.0131	0.0133	0.0132	0.0132

NEARSHORE ENERGY DENSITY AT SIGMA= 2.513

0.0000	0.0000	0.0000	0.0000	0.0000	0.0000	0.0000
0.0000	0.0000	0.0000	0.0000	0.0000	0.0000	0.0000
0.0000	0.0000	0.0000	0.0000	0.0000	0.0000	0.0000
0.0000	0.0000	0.0000	0.0000	0.0000	0.0012	0.0000
0.0000	0.0000	0.0012	0.0000	0.0042	0.0042	0.0005
0.0002	0.0000	0.0000	0.0065	0.0065	0.0004	0.0000
0.0009	0.0004	0.0000	0.0074	0.0000	0.0000	0.0000
0.0019	0.0080	0.0001	0.0081	0.0000	0.0000	0.0000
0.0036	0.0086	0.0014	0.0086	0.0000	0.0000	0.0002
0.0055	0.0090	0.0039	0.0090	0.0036	0.0000	0.0012
0.0067	0.0078	0.0061	0.0091	0.0046	0.0092	0.0037
0.0070	0.0073	0.0070	0.0075	0.0069	0.0079	0.0066
0.0071	0.0072	0.0072	0.0073	0.0073	0.0073	0.0073

NEARSHORE ENERGY DENSITY AT SIGMA= 2.827

0.0000	0.0000	0.0000	0.0000	0.0000	0.0000	0.0000
0.0000	0.0000	0.0000	0.0000	0.0000	0.0000	0.0001
0.0000	0.0000	0.0000	0.0000	0.0002	0.0002	0.0002
0.0002	0.0008	0.0006	0.0000	0.0010	0.0000	0.0000
0.0011	0.0015	0.0018	0.0000	0.0019	0.0019	0.0000
0.0019	0.0017	0.0024	0.0000	0.0027	0.0025	0.0001
0.0027	0.0021	0.0025	0.0002	0.0029	0.0031	0.0013
0.0031	0.0027	0.0031	0.0000	0.0024	0.0032	0.0022
0.0032	0.0031	0.0031	0.0032	0.0020	0.0033	0.0024
0.0032	0.0033	0.0031	0.0033	0.0028	0.0033	0.0028
0.0033	0.0033	0.0032	0.0033	0.0032	0.0033	0.0031
0.0033	0.0033	0.0033	0.0033	0.0033	0.0033	0.0033
0.0033	0.0033	0.0033	0.0033	0.0033	0.0033	0.0033

NEARSHORE ENERGY DENSITY AT SIGMA= 3.142

0.0000	0.0000	0.0000	0.0000	0.0000	0.0000	0.0000
0.0000	0.0000	0.0000	0.0000	0.0000	0.0000	0.0000
0.0000	0.0000	0.0000	0.0000	0.0000	0.0000	0.0000
0.0000	0.0004	0.0000	0.0000	0.0000	0.0000	0.0000
0.0000	0.0004	0.0001	0.0000	0.0000	0.0000	0.0000
0.0009	0.0005	0.0011	0.0002	0.0000	0.0011	0.0003
0.0012	0.0008	0.0012	0.0006	0.0012	0.0008	0.0003
0.0013	0.0010	0.0013	0.0009	0.0011	0.0006	0.0000
0.0013	0.0012	0.0013	0.0012	0.0013	0.0005	0.0013
0.0013	0.0013	0.0013	0.0013	0.0013	0.0013	0.0012
0.0013	0.0013	0.0013	0.0013	0.0013	0.0013	0.0013
0.0013	0.0013	0.0013	0.0013	0.0013	0.0013	0.0013
0.0013	0.0013	0.0013	0.0013	0.0013	0.0013	0.0013

ILLUSTRATIVE SAMPLE

COMPUTATIONS

The computer program has also been converted to suit the ICL 1906 machine at the Technical University at Braunschweig, West Germany. Field work has been conducted at the Island of Sylt in an attempt to verify the model. A set of sample computations are provided here. Data reduction is in progress and the results will be reported separately at a later date.

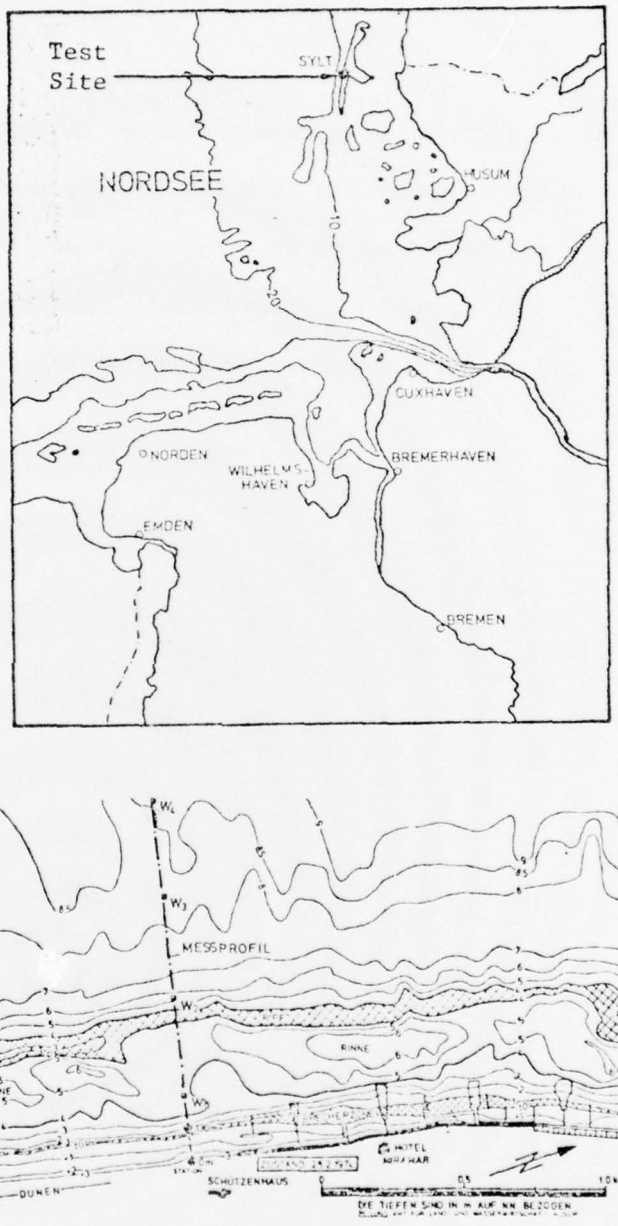

FIGURE 10 Location of Test Site (Island of Sylt/Germany, From Dette, 1974)

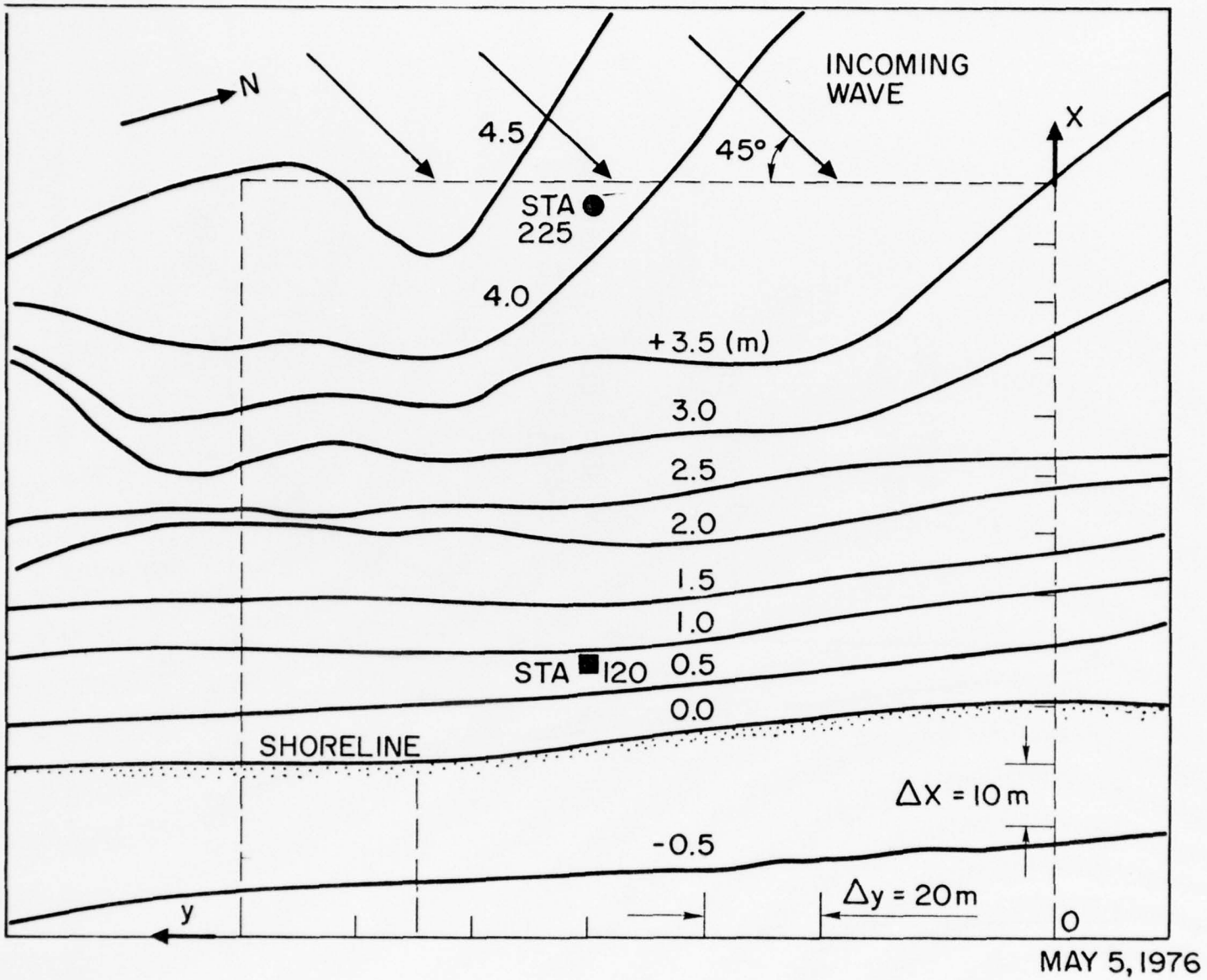

FIGURE 11 Nearshore Hydrograph at Test Site (Island of Sylt/Germany)

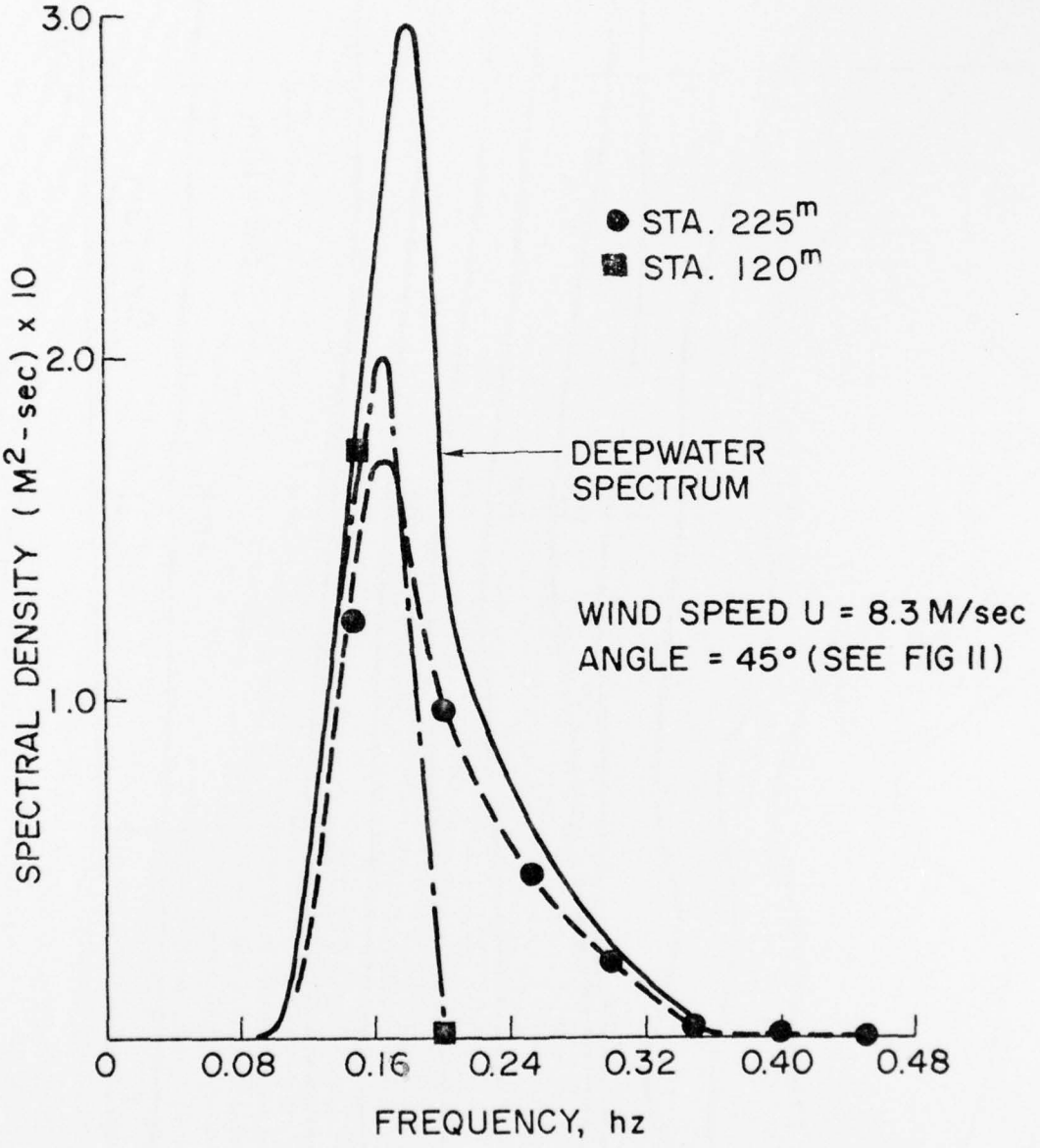

FIGURE 12 Spatial Variations of Wave Spectrum Over Irregular Bottom (Island of Sylt/Germany)

Security Classification

DOCUMENT CONTROL DATA - R & D

Security classification of title, body of abstract and indexing annotation must be entered when the overall report is classified

1. ORIGINATING ACTIVITY (Corporate author) Department of Civil Engineering University of Delaware Newark, DE 19711	2a. REPORT SECURITY CLASSIFICATION Unclassified 2b. GROUP Unclassified

3. REPORT TITLE

Computer Model for Energy Spectrum Transformation Over Irregular Bottom Topography

4. DESCRIPTIVE NOTES (Type of report and inclusive dates)

Technical Report,

5. AUTHOR(S) (First name, middle initial, last name)

Hsiang Wang; J. C. Shiau

(12) 54 p.

6. REPORT DATE July, 1976	7a. TOTAL NO. OF PAGES / 7b. NO. OF REFS
8a. CONTRACT OR GRANT NO b. PROJECT NO c. d.	9a. ORIGINATOR'S REPORT NUMBER(S) Technical Report No. 2 9b. OTHER REPORT NO(S) (Any other numbers that may be assigned this report) Ocean Engineering Report No. -9 TR-2

10. DISTRIBUTION STATEMENT

Distribution of this document is unlimited.

(15) N000 14-76-C-0342

11. SUPPLEMENTARY NOTES	12. SPONSORING MILITARY ACTIVITY Geography Branch Office of Naval Research Arlington, VA 22217

13. ABSTRACT

Based on the assumption that the wave energy associated with a narrow frequency band stayed within the band upon refraction, a numerical model based on finite difference method has been developed. This model, utilizing electronic computer, proves to be quite convenient to determine shallow water wave spectra at designated spatial locations of irregular bottom contours provided the deepwater wave spectrum is given. The model has been verified against analytical solution for case of two-dimensional parallel bottom contours and compared in good agreement with field measurement at location well beyond the surf zone.

DD FORM 1 NOV 68 1473 (PAGE 1)

S/N 0101-807-6811

407595 47

Security Classification

A-31408

(B)